UNIVERSITY OF OSLO
Department of Geosciences

Observed impact of aerosols on Arctic cloud emissivity

Master thesis in Geosciences
Meteorology and oceanography

Henrik Grythe

01.07.2011

Abstract

IPCC results indicate that the main bulk of uncertainties on global warming are within aerosol-cloud interactions. Based on observations, this thesis aims to measure how anthropogenic aerosol from mid-latitudes increase emissivity of clouds in the Arctic, thereby increasing Arctic surface temperatures.

Until recently this effect has been thought to be insignificant, but recent studies indicate that in the Arctic, many clouds may be susceptible to changes in emissivity. This is due to the presence of few CCN and low liquid water paths in the Arctic making clouds more sensitive. Therefore, this is a cliamtologically significant effect in Arctic regions (Lubin and Vogelmann, 2006).

With a long time series of measurements from Ny Aalesund (Svalbard), long term trends in clouds, climatology and aerosols are examined. A statistical approach is then used to investigate differences in longwave surface forcing from clean and polluted instances.

When investigating low clouds with small liquid water paths over Ny Aalesund a significant warming effect of 3.57 W/m^2 $[3.2 - 4.3]$ is found in the presence of high accumulation mode aerosols, compared to low accumulation aerosol concentrations. This is linked to the cloud droplets having a smaller effective radius, giving the clouds higher emissivity, and is comparable to recent observations based findings by (Garrett and Zhao, 2006; Lubin and Vogelmann, 2006).

Annual results show a potential significant surface forcing by what is recognized as a cloud emissivity effect.The actual annual surface heating of this effect is established to have a potential of $(0.24 - 0.29 W/m^2)$, which is the same order of magnitude as the modeledÂ results (Alteskjær et al., 2010), showing that the frequency of affectable clouds is probably as low as model results indicate. A decreasing trend in accumulation mode aerosol number concentrations are uncovered and the origin of the aerosols are investigated.

Results found in this study indicate that more specific instruments for observations of clouds are needed at Ny Aalesund., The cloud emissivity effect can, however, be measured with relatively simple low-maintenance instruments.

Acknowledgements

First of all I would like to thank my supervisor Terje Koren Berntsen for his support and well though guidance. Also my co-supervisor Jón Egill Kristjánsson should be thanked for his valuable input.

Of invaluable help throughout the work has been Johan Ström. For setting up connections, giving me a job, organizing trips to Ny Aalesund & Stockholm and generally helping me find my way in this complex path of this science.

Many people have supported me in collecting the various data from Ny Aalesund. From Norwegian Polar institute, Vigdis Lonar Barth. At Alfred Wegner Institute, Siegrid Debatin and Marion Maturilli have helped me a lot. In gathering the MPL data i would like to thank Masataka Shiobara for allowing me to use them and Judd W. Ellsworth (NASA) & Larry R. Belcher (NASA-MPLNET) for supplying the data. At Stockholmska Universitet the aforementioned J. Ström has helped with the aerosol data.

Helping me by answering questions through correspondence have T.J. Garrett, and many more have helped with correspondence that should have been mentioned. Also K. Alteskjaer have been helpful with the 1-D model.

A great thanks to Andrea Kanavin for helping me structure and for proofreading my far from perfect english.

Finally I'd like to thank Ada Gjermundsen, not just for her invaluable help in reading and discussions, but for listening to my rants and torments and also for being supportive and caring.

Contents

Chapter 1

Introduction

The World's northernmost settlement is Ny Aalesund at almost $79°N$. The t-shirts they sell sell at Ny Aalesund proudly proclaim an annual mean temperature of $-5°C$. 10 years ago this was true: at the turn of the millennium the annual mean temperature was $-5.2°C$. Since then there has been a steady trend of warming. Following this trend the predicted annual mean temperature in Ny Aalesund in 2011 is $-3.6°C$, a warming of $1.6°C$!

Today there is a virtually unanimous consensus among scientists that our planet is warming. Human activity is to varying degrees pointed to as the cause of this. In order to achieve a better understanding of how the climate is affected by these changes, both now and in the future, it is crucial to attain a more accurate research. By examining aerosol-cloud interactions in the Arctic region this thesis aims at providing a small piece to the large puzzle of how climate is affected by human activity.

1.1 Impact of aerosols on Arctic clouds

Growing awareness of Arctic warming has lead to invigorated research on Arctic clouds, and it has been found that Arctic clouds on average act to warm the region (e.g. Curry and Ebert (1992); Quinn et al. (2008)). Because of the active role of clouds have in forcing climate, improved knowledge of how Arctic clouds respond to human activities is important in order to understand the observed Arctic warming.

The Arctic region, in this thesis defined as the area north of the Arctic circle, will experience a more rapid change in surface temperatures than the global average as a result of global warming. This is due to strong regional feedback mechanisms such as diminishing sea ice and an earlier onset of snowmelt caused by warming which reinforces this regional heating. It is these mechanisms which make the polar regions especially exposed to climate variations (e.g. IPCC (2007)). The observed trend of Arctic warming at Ny Aalesund

(NYA) is by no means exceptional. Although observations in the Arctic region are limited to only a handful of stations, scattered far apart, warming trends are similar to that of NYA at all Arctic stations (e.g Overland et al. (2004)).

The reason observations are scarce in the Arctic is the harsh climate, as well as the remoteness of the region making it particularly inaccessible. Instruments at stations like NYA provide some insight into the Arctic atmosphere, and together with satellite observations findings from these instruments provide a basis for what is known of the Arctic climate. In the Arctic, as elsewhere, clouds are a major constituent of the climate. Observations of clouds, establishing theory and anlysis of cloud data are therefore important to understand the Arctic climate.

Clouds in general have a cooling effect on the climate. Clouds reflect and absorb incoming shortwave radiation, as well as absorb and emit thermal longwave radiation. The global net radiative effect results in a net cooling of both the troposphere and the surface. This is because, of the two, the shortwave effect is larger and is a cooling effect. In the Arctic, however, the high surface albedo of the Arctic snow and ice reduce the shortwave albedo effect of clouds. In addition only small amounts of shortwave radiation are available during the long Arctic winter. This means that the reflectiveness of incident sunlight on clouds is much less important here than at low and mid-latitudes. This leaves the Arctic more sensitive to the longwave radiative balance of the clouds.

Both shortwave and longwave radiative effects of clouds are affected by cloud microstructure, of which aerosols are an important part. Aerosols acting as cloud condensation nuclei (CCN) are thought to indirectly force the climate to cool on a global scale (e.g. IPCC 2007; Lohmann and Feichter (2005)). These radiative effects of aerosol-cloud interaction are commonly referred to as aerosol indirect effects (Lohmann and Feichter (2005)) and are summarized in figure 1. Aerosols act on clouds in several ways. In fact, together these aerosol-cloud interactions constitute the largest uncertainty in anthropogenic forcing in global climate models today (IPCC, 2007). Although the total impact of aerosol indirect effects are cooling globally, the impact is not necessarily cooling in the Arctic.

This thesis focuses on a longwave aerosol indirect effect, the cloud emissivity effect, which is not included in figure 1. This is an effect similar to the cloud albedo effect (Twomey (1977). The cloud albedo effect (see figure 1) describes how CNN increases the amount of solar radiation reflected by clouds. The cloud emissivity effect similarly consideres the cloud droplet number concentration (CDNC). In addition to changing the shortwave albedo, increased CDCN can also change the emissivity of the cloud. The reason this longwave effect is not included in most literature is that the emissivity of clouds are

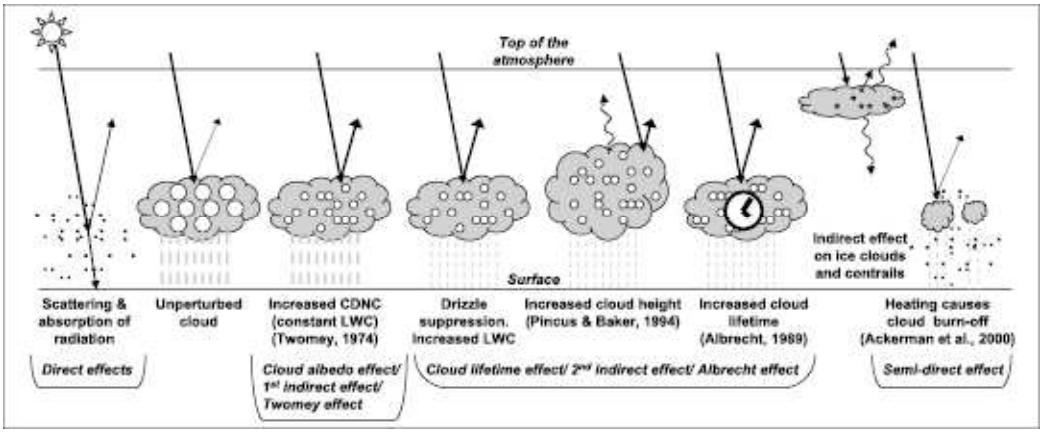

Figure 1.1: IPCC WG1 figure 2.10: "Schematic diagram showing the various radiative mechanisms associated with cloud effects that have been identified as significant in relation to aerosols. Black dots are aerosol, White circles are cloud droplet number concentration (CDNC), lines are shortwave radiation, waves longwave radiation and gray dashed is precipitation. The unperturbed cloud contains larger drops as only natural aerosols are available as cloud condensation nuclei (CCN)"(IPCC, 2007)

normally close to 1, so that it cannot increase due to changes in CDNC.

This longwave indirect effect may be important in understanding the changes in the energy balance in the Arctic due to anthropogenic influences. Based on measurements from Barrow (Alaska) Garrett and Zhao (2006) found that the estimated surface forcing accredited to first longwave indirect effect was $[3.3 - 5.2]\ W/m^2$ for frequently occurring clouds.

Also based on observations at Barrow, Lubin and Vogelmann (2006) found this effect to be a significant warming factor in the Arctic. On the other hand, a study utilizing a global climate model Alteskjær et al. (2010), indicated that the pan-Arctic effect was only $[0.1 - 0.85]\ W/m^2$; significantly lower than indicated by Lubin (2006) and Garrett and Zhao (2006). This show that research to date shows a lack of consensus regarding the significance of the cloud emissivity effect. The research conducted in this thesis aims at providing new data in order to account for these previous findings and increase our understanding of the cloud emissivity effect.

1.2 Aim and structure

For several years instruments on Svalbard have been measuring cloud atmospheric properties. The data gathered from Ny Aalesund includes ground based radiation measurements of longwave and shortwave fluxes, micropulse lidar (MPL) measurements of cloud and Planetary boundary layer (PBL)

properties and aerosol measurements from the Zeppelin station. The aerosol measurements include particle size distribution, number of condensation nuclei, and chemical composition. This thesis examines the Ny Aalesund data in a unique combination in order to establish if clouds above Ny Aalesund have a measurable indirect longwave effect. This research not only quantifies the longwave indirect for the clouds affected, but also aims to establish their occurring frequency. By doing this, this will be the first observation based estimate of the annual first indirect longwave effect. By tracing the aerosol back to their source it is also possible to establish the extent to which they are anthropogenic.

In the crucial task of understanding the Arctic responses by adding analysis of observational data from new locations is important in order to establish if the Barrow findings are general for the Arctic. By examining the results found, this thesis suggest that the apparent discrepancy between modeled and observed results are not in fact so large.

This thesis is broken up into six chapters. Following the introduction relevant theory (chapter 2) and previous research (chapter 3) is presented. After having provided a background for the research conducted, the methods and instruments used in this thesis are presented in chapter 4. Chapter 5 will present results and provide a discussion of the findings. Finally, chapter 6 provides a summary and conclusion.
ï»¿

Chapter 2

Theory

In this chapter,the theoretical grounds of the thesis are laid out. The principle aim of this section is to establish that there is a quantifiable cloud emissivity effect of aerosol. The backbone of this effect are the radiative transfer equations, which are first presented. Cloud properties and radiative effects are then discussed (section 2.1), followed by the calculations made by Garrett et al. (2002) based on empirical results (section 2.2).

The energy balance at the top of the atmosphere (TOA) is a driver for whether the temperature of both the surface and the atmosphere either warms or cools. The energy balance is a balance between the incoming solar (shortwave) radiation absorbed by the Earth and the outgoing terrestrial (longwave) radiation emitted from the Earth. This radiative transfer is the most important energy transfer in the atmosphere and at the surface, and makes radiation the principle component governing the temperature of the earth-atmosphere system (Hartmann, 1994).

Within the atmosphere and surface, the net flux of radiative energy through a plane surface (F_{net}), is given by the difference in radiative flux down ($\downarrow$) and up ($\uparrow$),where F is defined as positive downwards:

$$F_{Net} = F\downarrow - F\uparrow \quad [W/m^2] \tag{2.1}$$

The flux density emitted by an object is proportional to its temperature (T) and is given by the Stefan-Boltzmann relation:

$$F = \epsilon\sigma T^4 \tag{2.2}$$

where, for a given wavelength (λ), the emissivity, ϵ_λ, equals the absorptivity, A_λ. A blackbody has emissivity equal 1 for all wavelengths, and a non-blackbody has at least some wavelengths where emissivity (absorptivity) is smaller, so that the energy emitted (absorbed) by a non-blackbody is less than that of a blackbody. In addition to absorption, incident radiation is also reflected or transmitted, so that by conservation of energy $A + t + r = 1$ where r is reflectivity and t transmissivity.

For direct shortwave radiation from the sun, the radiative transfer equation can be given by:

$$F(z) = F_{TOA} e^{-\tau(z)/\mu_0} \tag{2.3}$$

Where $\tau(z)$ is optical depth form TOA to z and μ_0 is the zenith angle of the sun. At the surface τ is then the optical depth of the atmosphere. τ is then the combination of the absorption and reflection by the atmosphere. The presence of clouds alter the optical properties of the atmosphere drastically, compared to how gases and particles vary by the absorbance and reflectance of radiation.

Longwave radation emitted by the Earth and the atmosphere undergo both absorption and emission processes simultaneously. Thus, the equation for longwave radiative transfer also includes a source term:

$$I_\lambda(s_1) = I_\lambda(0) e^{-\tau(s_1,0)} + \int_0^{s_1} B_\lambda[T(s)] e^{-\tau(s_1,0)} k_\lambda \rho ds \quad [W\mu^{-1}m^{-1}sr^{-1}m^2] \tag{2.4}$$

In equation 2.4, s and s_1 is the distance travelled by the beam and $B_\lambda(T)$ is given by the Planck function. I_λ is the intensity and the flux density can be given as the integrated intensity over an solid angle Ω:

$$F = \int_\lambda \int_\Omega I_\lambda \cos(\theta) d\Omega d\lambda \tag{2.5}$$

2.1 Clouds

Clouds affect the climate by absorbing and emitting thermal longwave radiation, as well as by absorbing and reflecting solar shortwave radiation. The presence of a cloud will therefore alter the radiative flux in the atmosphere. A cloudless atmosphere is highly transient to shortwave radiation. Most solar shortwave radiation that enters at TOA are transmitted or reflected and only very little is absorbed by the atmosphere.

In the presence of clouds, the dominating radiative effect is the cooling effect: More shortwave radiation is reflected so that less energy is received by the earth-atmosphere system. On the other hand, the absorption and emission of longwave radiation by clouds leads to a warming of the atmosphere and the surface. However, this effect is in general less than the shortwave cooling. As a result, clouds on average act to cool both the troposphere and the planetary surface.

Cloud forcing at the surface (SCF) can be seen as the sum of the longwave (LW) and shortwave (SW) net surface effect:

$$SCF = SCF^{SW} + SCF^{LW} \quad [W/m^2] \tag{2.6}$$

The effect of the absorption by clouds on surface temperature is determined by the temperature of the clouds, surface and atmosphere. Surface forcing associated with clouds is determined by the net flux difference in the presence of clouds to that of a clear sky:

$$SCF = F_{Net}^{cloud} - F_{Net}^{clear} \tag{2.7}$$

At the surface this can be seen as the net downward flux of energy to the surface (equation 2.1) so that the surface cloud forcing (SCF) can be determined by combining 5.1 and 2.1:

$$SCF = F\downarrow_{cloud} - F\uparrow_{cloud} - (F\downarrow_{clear} - F\uparrow_{clear}) \tag{2.8}$$

2.1.1 Arctic clouds

In the Arctic the dominant radiative effect is in the longwave. This is because the reflective shortwave effect of clouds to some extent is negated in the Arctic by the high surface albedo[1]of the snow and ice that also reflect a large proportion of radiation. During winter there is very little incoming solar radiation and in this period the only radiative effect of clouds are in the longwave.

The growing awareness of the Arctic warming and research of Arctic effective CCN, show that improved knowledge of how Arctic clouds respond to human activities is therefore important in order to understand the observed Arctic warming. The clean Arctic air has very few primary sources of aerosol. The Arctic experiences a large influx of aerosol, especially during November- April (e.g Martin et al. (2011); Garrett et al. (2004)). It is also cold, so that more clouds have lower liquid water paths (LWP's) than in warmer regions. The combination of these two factors make many clouds susceptible to changes in emissivity. Thus, a longwave emissivity effect may have larger effect in the Arctic than elsewhere.

2.2 Cloud emissivity effect

Cloud albedo effect

In 1974-77, S. Twomey (Twomey, 1977) suggested that an increase in the CCN concentration, resulting from an increase in the aerosol concentration of the ambient air, would lead to an increase in the cloud optical depth and

[1] ''Albedo is defined as the ratio of the amount of flux reflected to space of the incoming solar radiation'' (Liou, 2002) This is the proportion of the incoming solar radiation that is reflected back to space without being absorbed.

the albedo of liquid clouds. More, but smaller, cloud droplets increase the surface to volume ratio of liquid water in clouds, which increases the albedo. This is known as the Twomey effect, the first indirect climatic effect of aerosols, or the cloud albedo effect (success has many fathers).

While increased cloud droplet number concentration (CDNC) changes the reflectivity of the shortwave radiation in clouds, it can also change the radiative properties of clouds for longwave radiation. An increase in CDNC can cause increased emissivity for thin clouds, which in turn causes an increase in the upward and downward radiation emitted by these clouds. This effect is mainly seen in thin clouds due to the sharp increase in the emissivity with cloud thickness.

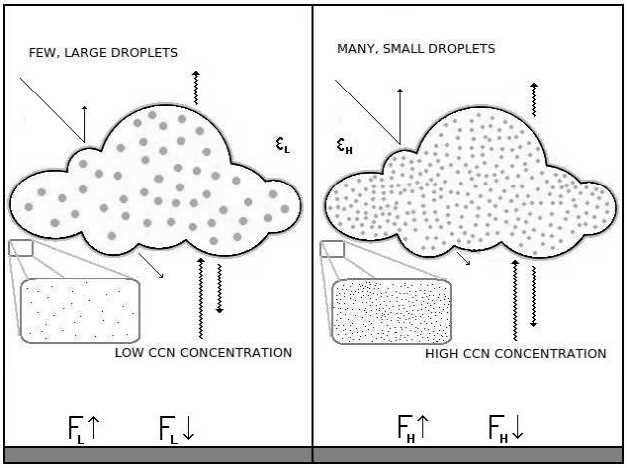

Figure 2.1: Schematic of how high CCN concentrations affect droplet numbers and size. More aerosol (and thus CCN) leads to higher CDNC and this effects not only the shortwave (top) but also emissivity $\epsilon_L < \epsilon_H$. Higher emissivity leads to more absorption ($\epsilon = A$) of thermal radiation from the surface. The longwave fluxes from the cloud is increased as a result of the increased emissivity.

Emissivity and optical depth of clouds

Clouds can have either a net positive forcing (warming) or a negative forcing (cooling) effect on the surface, depending on a number of factors. Some of these factors are; the temperature of the cloud relative to the temperature of the surface; the thickness of the cloud; the location and coverage of the cloud; the time of day; etc. Regardless of the net forcing of a cloud, an instantaneous increase in cloud emissivity will nearly always be a positive surface forcing. An increase in cloud emissivity may have a negative surface

forcing only if the flux of longwave radiation downwards (LWD)[2] is larger than the flux of longwave radiation upwards (LWU)[3] at the location of the cloud, which only very special meteorological conditions can produce..

The aim of this section is to show that there can be an increase in cloud emissivity as a result of changes in cloud droplet distributions for liquid clouds. In order to determine the effect of increased aerosol concentration, and the resulting increased CDNC, it is necessary to look at the sensitivity of cloud emissivity to the microstructure of the cloud.

If we only consider longwave radiation, multiple scattering can be ignored, and the emissivity of a cloud can be approximated by:

$$\epsilon = 1 - e^{-\beta_{abs}\tau} \tag{2.9}$$

where β_{abs} is the diffusivity factor and τ is the optical depth of the cloud regarding absorption given by (Garrett et al., 2002):

$$\tau = \pi \int_0^h \int_0^\infty Q_{abs}(r, z, \lambda) r^2 n(r) dr dz \tag{2.10}$$

Here Q_{abs} is the efficiency at which droplets absorb radiation dependent on droplet radius r, the vertical thickness of the cloud z, and wavelength λ. The integral $\int_0^\infty dr$ is the droplet distribution, where $n(r)$ is the droplet distribution function. Equation 2.10 is inconvenient to work with, therefore by assuming the cloud to be vertically homogeneous we can write τ as (Liu (2002)[4]):

$$\tau = \pi h \int_0^\infty Q_{abs}(r, \lambda) r^2 n(r) dr \tag{2.11}$$

Using the actual droplet distribution is impractical. Therefore, in order to ease calculations, the effective radius can be used as an approximation for the droplet distribution. The effective radius (r_e) of the droplet is a weighted mean of the size distribution of cloud droplets. r_e represents the radius of uniform droplets having the same optical properties as the droplet distribution of the cloud and is given by:

$$r_e = \frac{\int_0^\infty \pi r^3 n(r) dr}{\int_0^\infty \pi r^2 n(r) dr} \tag{2.12}$$

Using equations 2.12 with 2.11 the optical depth τ can be written as:

$$\tau \simeq \pi Q_{abs}(r_e, \lambda) r_e^2 N h \tag{2.13}$$

[2]here LWD = $F\downarrow$
[3]here LWU = $F\uparrow$
[4]eq: 7.3.13c

where N is the CDNC. Using this expression for τ, the emissivity can be given by:

$$\epsilon = 1 - e^{-\beta_{abs} Q_{abs}(r_e,\lambda) N h \pi r_e^2} \tag{2.14}$$

The diffusivity factor β_{abs} must be determined empirically. Garrett et al. (2002) estimated by a series of measurements that for Arctic clouds $\beta_{abs} = 1.8 \pm .2$.In the same paper, 7th order polynomials were fitted for several wavelengths for $\beta_{abs} Q_{abs}$. Of these a wavelength of $11\mu m$ was found to be the most significant for Arctic temperatures, and was applied when calculating sensitivities.

The sensitivity of the cloud emissivity

The sensitivity of the cloud emissivity, S_{LW}, can be quantified through $\frac{\partial \epsilon}{\partial N}$. When differentiating it is assumed that r_e is independent of N. This approximation, however, is not obvious and may be considered poor. Nonetheless, it is necessary for these calculations.

$$\frac{\partial \epsilon}{\partial N} = S_{LW} = \beta_{abs} Q_{abs}(r_e, \lambda) h \pi r_e^2 e^{-\beta_{abs} Q_{abs}(r_e,\lambda) N h \pi r_e^2} \tag{2.15}$$

The absorption efficiency Q_{abs} has been shown to have a strong dependency on the relationship r_e/λ. If the ratio r_e/λ is small, $Q_{abs}(r_e, \lambda)$ is proportional to ar_e, and if the ratio is large, $Q_{abs}(r_e, \lambda) \simeq 1$.

For a small r_e/λ ratio, using $Q_{abs}(r_e, \lambda) = ar_e$, the sensitivity can be written as

$$S_{LW} = \beta_{abs} a \pi r_e^3 h e^{-\beta_{abs} h a \pi r_e^3 N h} \tag{2.16}$$

For a large r_e/λ ratio, using $Q_{abs}(r_e, \lambda) = 1$, this becomes

$$S_{LW} = \beta_{abs} \pi r_e^2 h e^{-\beta_{abs} \pi r_e^2 N h} \tag{2.17}$$

In figure 2.2, the relationship between the sensitivity, N and emissivity in 2.15 is shown using empirically calculated values for $Q_{abs}(r_e, \lambda = 11)$ and β_{abs}.

To get a relation between N and r_e the expression for liquid water path (LWP) can be used. LWP is a measure of the liquid water content (LWC) in an air column of height h.

$$LWP = LWC \times h = h\frac{4}{3}\pi\rho_l \int_0^\infty r^3 N(r)dr = \frac{4hN\pi\rho}{3}r_e^3 \tag{2.18}$$

where ρ_l is the density of water.

Using equations 2.18, 2.15 and the empirical calculations of Garrett et al. (2002) to estimate $\beta_{abs}Q_{abs}$, one can see how both r_e and S_{LW} change with N and LWP (see figure 2.3 and figure 2.4).

Figure 2.4 shows that clouds with small LWP and few drops are the most sensitive to changes in CDNC. The emissivity of a cloud (figure 2.2) with few droplets (N) changes more than for a cloud of the same LWP, but with more droplets. Similarly the emissivity changes more for a cloud of low LWP ($< 50g/m^2$) than a cloud of large LWP ($> 50g/m^2$). This is of course depending on the vertical height (h) of the cloud. The most sensitive clouds (figure 2.2 and 2.4) have few droplets and a relatively low LWP.

2.3 Other aerosol effects

There are additional effects from increased CDNC. These are cloud lifetime effects and increased vertical height of clouds (figure 1.1). Cloud lifetime effects of increased CDNC, above a fixed position observation point, would

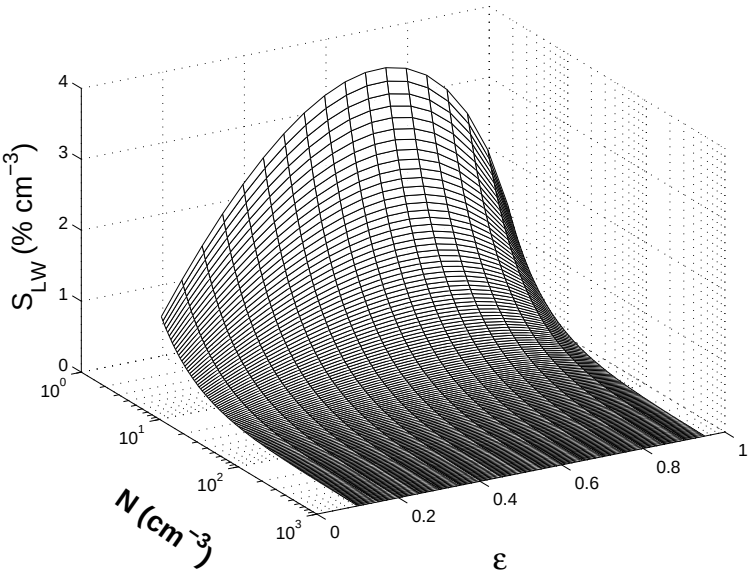

Figure 2.2: Sensitivity to changes of the number of droplets N for clouds with different emissivity. Sensitivity is for when increasing the droplet concentration with 1 per cm^3. Clouds with less than $100drop/cm^3$ are especially sensitive.

become evident with more observations of clouds with high CDNC compared to clouds with fewer CDNC. The reason clouds with large CDNC would be more frequent is that having a larger CDNC decreases the rate at which precipitation is formed. With a decrease in r_e the accumulation efficiency of raindrops in the cloud decreases. The sign of forcing of this effect is tied to the net forcing of the cloud, so that for a cooling (warming) cloud this effect would be a cooling (warming) effect.

Increased CCN levels may also increase cloud LWC and cloud vertical extension (Pincus and Baker, 1994; Albrecht, 1989). These effects increase the longwave downward flux and is a positive forcing in the longwave. Depending on the observation technique, these effects may be hard to distinguish from the altered radiative properties of the cloud emissivity effect. The method described in chapter 4.3, provides a way in which it is possible to distinguish cloud emissivity effects from other possible longwave effects.

Thus far, this chapter has presented is the theory of cloud emissivity effect. The radiative equations necessary to arrive at the cloud emissivity effect were first presented, along with the radiative influence of clouds in general and in the Arctic. The bulk of this chapter has described the empirical results of Garrett et al. (2002) on measured emissivities of Arctic clouds. Figures 2.2, 2.3 and 2.4 show that clouds with few droplets and low LWP's are the

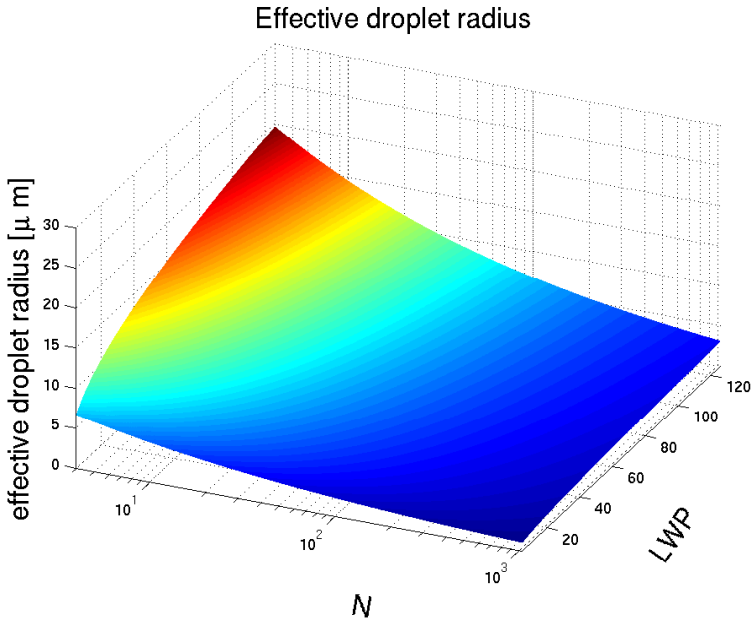

Figure 2.3: Dependency of effective radius on LWP and the number of droplets N. The figure shows the sensitivity of a cloud of vertical extent of 500m, giving the cloud a LWC of $0.03 - 0.5 g/m^3$ More droplets and less water makes each droplet smaller and makes its radius decrease.

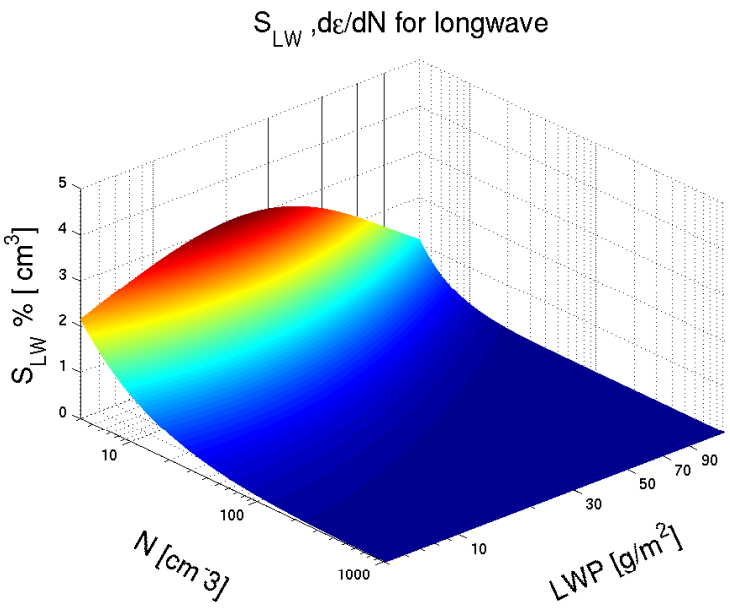

Figure 2.4: Sensitivity of cloud emissivity for changing the number of droplets with 1 cm^{-3} given in percentage, for the same cloud as figure 2.4.

most sensitive to changes in emissivity. The final section will describe some additional indirect effects of clouds that that are closely connected to the emissivity effect.

2.4 Cloud droplet nucleation

Aerosols are commonly defined as all solid particles and liquid droplets suspended in the atmosphere of sizes ranging from $\sim 0.01\mu m$ to $20\mu m$ in radii (Chen et al., 2007). Besides size variation, aerosols have a number of properties such as chemical composition, hygroscopicity, density and shape. All natural aerosols have their source near the surface. They originate from sea and land as sea-spray, dust or carbonate materials (primary production), or by chemical and physical processes of gases within the atmosphere (secondary production). Added to the natural concentration of aerosol comes the anthropogenic emissions, which contribute roughly 15% of the atmospheric aerosol mass (Seinfeld and Pandis, 2006).

In the ice-covered Arctic there are few primary sources of aerosol and few anthropogenic sources. Therefore, the Arctic, together with Antarctica, has on average lower aerosol concentrations than most regions. This is important with regard to cloud the emissivity effect, because having fewer CCN leads to formation of clouds with a lower CDNC. These clouds are therefore more

susceptible to a cloud emissivity effect (figure 2.2).

Most aerosols are potential CNN. When air saturation in an air parcel is increased, water vapor tends to attach itself to aerosols that are hygroscopic. Usually, when the air is just above saturation, in terms of a plane surface of water, small droplets will reach their critical radii and grow without losing energy. This radius is dependent on the mass of the aerosol and will be smaller for an aerosol of greater mass. This radius is also dependent on the aerosol chemistry (figure 2.5).

The initial growth of droplets formed on CCN can be described by its KÃ¶hler curves:

$$\frac{e'}{e_s} = exp(\frac{2\sigma'}{n'kTr})(1 + \frac{imM_w}{M_s(\frac{3}{4}\pi r^3\rho' - m)})^{-1} \tag{2.19}$$

Here r is the droplet radius, e' is the saturation pressure on the droplet, e_s is the saturation pressure to a plane surface of water, and i the number of ions per molecule of solution[5]. m is the mass of the solvent, M_w the molecular weight of water and M_s the molecular weight of the solution so that ρ' is the density of the drop. σ is the surface tension given in J/m^2, k is the Boltzmanns' constant $J/(K * mol)$, T is the temperature of the drop and n' the number of molecules per litre of the drop. The KÃ¶hler equation (2.4) can be used to determine whether a droplet is activated or not.

The critical droplet radius $r*$ and supersaturation $S*$ that marks the size a droplet change, from needing a net influx of energy to grow, to growing without energy input (activated droplet) is:

$$r* = \sqrt{\frac{3b}{a}} \tag{2.20}$$

$$S* = 1 + \sqrt{\frac{4a^3}{27b}} \tag{2.21}$$

Here $a = \frac{2\sigma'}{nkT}$ and $b = \frac{3imM_w}{4\pi r^3\rho' - m}$. Figure 2.5 show that the mass of the CCN is dominating, but clearly not the only influence in whether a drop is activated or not.

The theory of cloud emissivity effect, as well as other indirect effects of clouds associated with the emissivity effect, has been accounted for in this chapter. This was done in a context of Arctic clouds. The following chapter will go on to present relevant research regarding this theory.

[5]In figure 2.5 this is 2 for NaCl and 3 for ammonium sulfate.

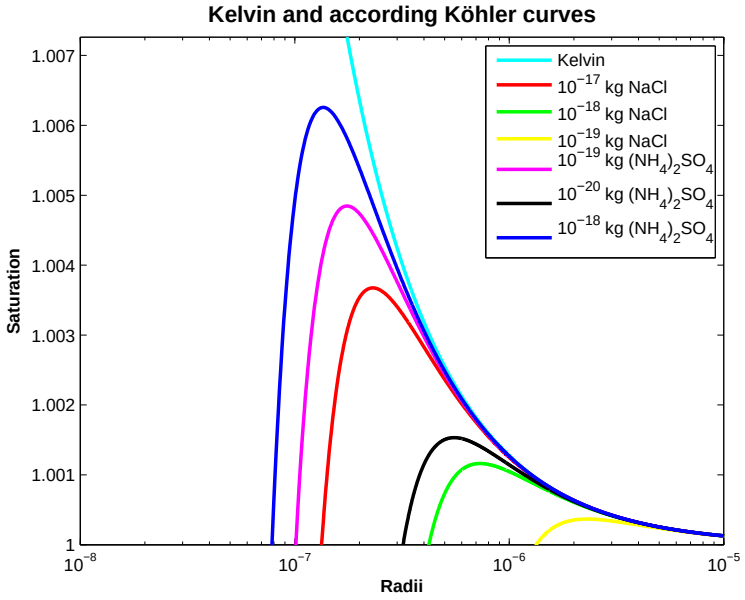

Figure 2.5: Graph showing droplet activation of NaCl, natrium chloride, and $(NH_4)_2SO_4$, ammonium sulfate, CCN's of different mass. Graph show that both the mass (and hence size) and CCN chemestry determines the saturation needed to activate a droplet. The dominating being mass. Peak in curves are criticla radii and saturation.

Chapter 3

Relevant research

For a long time aerosol-cloud interaction studies were somewhat limited by observations being hard to procure. As instruments have continued to improve, so has our ability to observe these mechanisms. Today scientists have access to long term observations of both aerosol and cloud microstructure. This has led to more attention on indirect effects of aerosols.

In order to properly determine the annual Arctic cloud emissivity effect of anthropogenic aerosols it is important to observe the local effect above an observation station, as well as to estimate the frequency of thin clouds that can be affected, and to find anthropogenic aerosol levels in the Arctic. Both observational studies and model based studies therefore provide important information needed to determine the annual Arctic longwave indirect effect. This chapter will therefore present observational studies and model based studies that study Arctic longwave indirect effects. Following this, research providing grounds to make annual predictions will be presented.

3.1 Observational studies

In the Arctic there are still few observations, and only a handful of sites provide long term measurements of aerosol and cloud microstructure. This is largely due to the cold and harsh climate and desolate conditions making operation of delicate instruments a challenging task.

Garrett and Zhao's (2006) paper "Increased Arctic cloud longwave emissivity associated with pollution from mid-latitudes" estimates the increased cloud longwave forcing due to increased emissivity under thin greybody clouds to be between $[3.3 - 5.2]\ W/m^2$, resulting from increased anthropogenic aerosol levels.

The Atmospheric Radiation Measurement programme (ARM) station and the Climate Monitoring Diagnostics Laboratory (CMDL) near Barrow, Alaska

has provided a long term dataset for cloud microphysics. This enabled Garrett and Zhao (2006) to retrieve ϵ_{cloud}, LWP and effective droplet radius (r_e) distributions . Using these data together with meteorological data enabled them to isolate 9440 5 min long samples of thin single layer clouds with cloud tops lower than 1500m over a 4 year period (2000-2003).

Garrett and Zhao (2006) compared lower (clean) and higher (polluted) quartiles of light scattering cross sections σ under the assumption that CCN is correlated to σ, to procure the forcing of $[3.3 - 5.2]\ W/m^2$. They found that about 60% of the samples had high pollution levels as a result from long-range transport.

In a study by Lubin and Vogelmann (2006) an Atmospheric Emitted Radiance Interferometer (AERI) instrument at the same location in Barrow, Alaska was combined with aerosol data and cloud microstructure observations to examine the aerosol-cloud interactions. From the AERI measurements, with a spectral resolution of $1cm^{-1}$ it is possible to directly retrieve r_e and LWP because the radiance of a clouds r_e and LWP shows sensitivity in different wavelengths. From the full 6 year dataset, measurements of thin single layer clouds were selected and subsequently, based on temperature soundings, conditions preferable to liquid water were selected. Quartiles of high and low CCN cases were selected and showed significant difference for r_e.

Sorting the 2379 low CCN cases and 5164 high CCN cases in LWP bins the mean difference in downwelling hemispheric LW flux for equal bins was found to be 3.4 W/m^2 the high CCN cases being the larger. Without any LWP, CBH or seasonal adjustments the mean difference was found to be 8.2 W/m^2 between the high and low CCN cases.

Despite using different methods, results from both studies suggest that longwave indirect effects significantly contribute to Arctic surface forcing. Their results imply that the magnitude of longwave indirect effects may be as large, or larger than, other aerosol radiative effects.

3.2 Modelled results

Both these studies considers an instantaneous surface forcing in a localized region, not a TOA global forcing. The results shown in observational studies should therefore be considered to show that the magnitude of cloud emissivity effect is signficant. Model based studies have an advantage in allowing for the investigation of radiation on all levels and in all scales of the atmosphere. It is therefore interesting to consider whether a global model provide the same implications as observational studies do.

A more recent study by K. Alteskjaer (Alteskjaer et al., 2010) uses a global climate model (CAM Oslo) to look at the annual net radiative effect of aerosol-cloud interactions over the whole Arctic region. The annual cloud emissivity effect of anthropogenic aerosols for the Arctic is estimated to $0.55 W/m^2$ $[0.1 - 0.85]$. This is about one order of magnitude less than what was observed in Garrett and Zhao (2006); Lubin and Vogelmann (2006).

This difference may have several causes. While Garrett and Lubin investigated specially selected cases, where clouds were thought to be sensitive, Alteskjaer's (2010) study models the annual effect for the entire region. Furthermore, Alteskjaer (2010) tested the CAM Oslo model's physics with a 1-D model where the parameters used were those of Garrett and Zhao (2006) for r_e and LWP for polluted and clean conditions. While Garrett and Zhao (2006) found changes in cloud forcing to be $[3.3 - 5.2]$ W/m^2 between polluted and clean clouds, the simulated changes of the model was $[2.1 - 2.6]$ W/m^2 run for July and January. This suggests that the model's physics slightly underestimates the changes in cloud forcing for these r_e.

While the CAM Oslo model shows signs of underestimating cloud cover and overestimating LWP compared to observations, both of which would tend to decrease the longwave indirect effect; the results of this research is a strong indication that both Lubin and Vogelmann (2006) and Garrett and Zhao (2006) papers may not be applicable to a regional and annual scale. A further discussion of the causes for this difference in findings is found in chapter 5.

Thus far, observational studies and model based studies that study Arctic cloud emissivity effects have an estimate of surface longwave indirect. In order to attempt to generalize these local observations, it is important to consider studies looking at properties of arctic cloud cover.

3.3 Properties of Arctic cloudcover

In order to estimate annual forcing, it is imperative to know how often clouds that are sensitive to longwave emissivity changes come about. There has been some progress on assessing this.

During the Surface Heat Budget of the Arctic ocean (SHEBA) campaign in 1997-98, temporal distribution of clouds, their height, phase and vertical distributions were measured at a drifting site on the Arctic ice sheet. At this site depolarized lidar was combined with radar to give an accurate description of the physics of the atmosphere above.

The annual cloud cover was found to be about 85%, with a maximum of nearly complete cloudiness in fall and a tendency for a clearer sky in winter

than in summer. Annually $\sim$ 75% of the detected clouds contained water. During summer nearly all clouds detected contained water. During winter the percentage decreased by a minimum of $\sim$ 25% in December (Initieri et al., 2002b). For the most part of the year, single layer low clouds were found to be dominating. An exception to this being the summer months where many instances of high cirrus in multiple layers often lay over clouds beneath (Initieri et al., 2002b).

Cloud-Aerosol Lidar and Infrared Pathfinder Satellite Observations (CALIPSO) was launched in 2006 and has since then provided global data on aerosols and cloud properties, making it possible to study cloud properties up to $82°N$[1]. The on-board lidar observes optical and vertical features of cloud cover over the Arctic region here defined as 67-82°N.

Four year data from CALIPSO shows that for thin clouds with cloud base below 2km is dominated by liquid water throughout the year, and only to some extent were low clouds found to hold ice. Annually these data show a cloud cover of $\sim$ 75%, of which about half was single layer clouds (Devasthale et. al; 2010).

CALIPSO data point to a relatively high occurrence of optically thin low clouds that could be susceptible to changes in their emissivity with the introduction of more aerosols. Also a large proportion of the low clouds were mix-phased or liquid.

3.4 Arctic aerosol sources

Finding out where aerosols measured at NYA (Zeppelin) come from is important to find the anthropogenic contribution to Arctic aerosols. Also comparison with other Arctic stations in terms of origin of the aerosols measured there can indicate if the Zeppelin measurements are general for the Arctic or not.

Hirdmann et al. (2011) studied long term trends of aerosols at three different Arctic stations, one of which was the Zeppelin station near NYA. This study used the Lagrangian dispersion model FLEXPART, run backwards in time using ECMWF[2] operations analyses, to evaluate a source-receptor-relationship between source regions and aerosols measured at the Arctic stations.

Cluster analysis was applied to define 9 geographical regions of the Earth of which the 4 though most important regions were chosen for each station. For Zeppelin, North America (NA), Western Norther Eurasia (WNE), Eastern

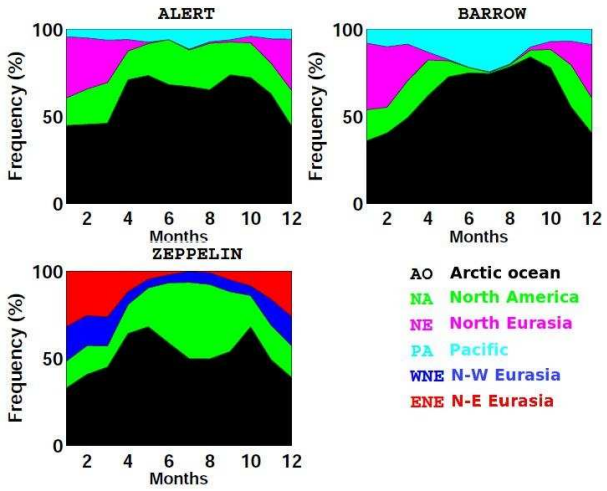

Figure 3.1: Fig. 10 Hirdmann et al. (2011) "The frequencies of the transport clusters as function of the month of the year for Alert (upper left), Barrow (upper right) and Zeppelin (bottom left)"

Norther Eurasia (ENE) and the Arctic ocean (AO) were chosen.

Aerosol observations at Zeppelin are the same as those presented in this thesis' section 5.1. The current decline in observed aerosol masses at Zeppeling was attributed to decreases in pollution levels in WNE and NA. While finding distinctly differences in seasonal origins of aerosols (figure 3.1) there was no long-term trend of changes to this pattern for Zeppelin.

This chapter has provided an overview of relevant research needed to determine annual Arctic longwave indirect effect of anthropogenic aerosols based at observations around NYA . Observations measuring local effects above an observation station have been presented, and a relevant model study has been reviewed. Relevant research looking at cloud cover in the Arctic has provided grounds on which to estimate the frequency of thin clouds that can be affected. Finally, an investigation on the origins of anthropogenic aerosols in the Arctic has been reviewed.

[1]http://www-calipso.larc.nasa.gov
[2]European Center for Medium range Weather Forcasts

Chapter 4

Instruments & Methods

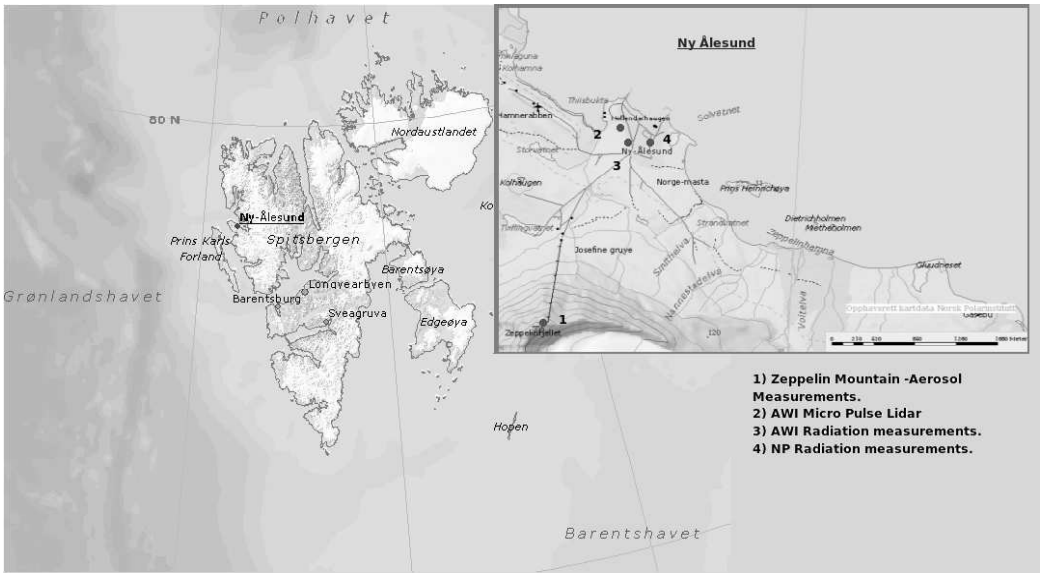

Figure 4.1: Map of Svalbard archipelago. Inset Ny Aalesund and surrounding area including instrument location around research base. The distance between radiation measurements and aerosol measurements are about 1200m, with aerosol measurements conducted at 476m and MPL and radiation at 11m altitude.

Ideally placed for Arctic observations the research base Ny Aalesund on Svalbard (figure 4.1) was established in 1964 on the remains of an old coal mining community. Far away from any sources of pollution, in the deep Arctic ($78°55'N$ $11°56'E$), it has been used as a launch base for Arctic expeditions, as well as a research station.

Among the many research facilities is the Norwegian Polar Institute (NP) and the German Alfred Wegner Institute (AWI), both conducting atmospheric measurements. Also present is University of Stockholm (SU) and the Norwegian Institute for Air Research (NILU). Together NP, AWI and SU

provide all the data used in this thesis. The following chapter will present the instruments used to obtain the dataset, as well as the methods used to examine it.

4.1 Instruments

The dataset used is a combined set of data measuring three principal atmospheric properties: radiation (NP, AWI); cloud properties (AWI) and aerosol (NILU). The longest continual observations available of these three properties is the radiation measurements. These have been collected since 1974 by NP, and more recently by AWI. In 1999 AWI installed a Micro Pulse Lidar (MPL) for cloud measurements, and since 2000 a Condensation Particle Counter (CPC) have been in operation to measure aerosol properties.

There are also numerous other measurements conducted in Ny Aalesund; both atmospheric, cryospheric and oceanic. General meteorological properties are routinely reported from both NP and AWI for forecasting and rawinsondes are released every 12th hour. The following section focuses on the instruments utilized, how they are operated, their reliability, as well as what the different instruments measure.

In order to ensure the quality of data retrieved from each instrument logged, an extensive filtering of the raw data is performed. Since this process have not been performed for some of the instruments before, a description of the processes involved to get from raw data to physical units for the different instruments is included. As close as possible the calculations done is in accordance with WMO specifications for measurements and calibration (Vuerich, 1999).

The make and model of instruments

1. Kipp & Zonen CHP 1 Pyrheilometer -For measurements of direct shortwave irradiance at NP
2. Eppley Normal Incidence Pyrheilometer (NIP) -For measurements of direct shortwave irradiance at AWI
3. Kipp & Zonen CM11 Pyranometer -Diffuse and global hemispheric shortwave irradiance
4. Eppley Precision Infrared Radiometer (PIR) Pyrgeometer -Longwave hemispheric irradiance
5. Condensation Particle Counter (CPC) model TSI 3010 -Parametrized size aerosol counter
6. Micro-pulse lidar (MPL) (NASA upgraded SESI model) -Gives among other things CBH and CTH

Figure 4.2: Left: Eppley (PIR) pyranometer in lab for calibration. Right: Pivoting suntracker at the roof of NP building with pyranometer (CM11) for diffuse shortwave measurements and a pyrheilometer for direct. Zeppelin mountain can be seen in the background (upper right)

4.1.1 Radiation instruments

There is a double set of radiation measurements. Both AWI and NP measure radiation on sites which are in close proximity to each other, location 3 & 4 respectively in figure 4.1. AWI has a rack supporting all radiation instruments, standing clear of all interference from buildings on the tundra from their main building. A similar rack support most NP radiation instruments, although they also have a roof terrace with substantial instrumentation.

For the instruments facing towards the upper hemisphere, location is not thought to significantly influence measured quantities. However, for direct sunlight this may not be true, since these instruments have large local variations over short timespans. The major discrepancy may be found in albedo measurements (SWU) where local surface condition may vary significantly over short distances. This is especially true in periods when snowcover is incomplete.

Pyranometer

Kipp & Zonen CM11 was used for all hemispheric shortwave measurements. According to World Meteorological Organization (WMO) a pyranometer is designed for measuring shortwave irradiance on a plane surface (Vuerich, 1999) The CM11 pyranometer consists of a thermophile kept safe by two domes that are 97-98% transient for shortwave radiation in the spectrum $285 - 2800nm$. The black thermophile absorbs radiation and converts this into electric resistance, which is calculated within the sensor, to an electric signal output representing the absorbed radiation. The instrument is wavelength independent, because it absorbs frequencies in all bands the dome is transient for.

The flux density (E_{SW}) for the hemisphere the instrument is directed at

$$E_{SW} = U_{emf}/S \quad [W/m^2] \tag{4.1}$$

Where S is the sensitivity given in $\mu V/Wm^{-2}$ and U the recorded instrumental output value measured in μV. The instruments are calibrated by being exposed to a source of known radiative energy in its sensitivity band. The signal from the instrument is then tuned so that the electrical pulse of this signal corresponds to the exposed energy, making S an instrumental value.

This instrument has a very accurate reading when ideally placed. It is, however, very sensitive to inaccurate placement and if it is not level this may influence the results. AWI has a 3% inaccuracy estimation for their minute average observations, increasing with zenith angles[1]. There is a second significant source of error that may influence recorded values sporadically, namely precipitation and drifting snow, which is hard to eliminate completely.

CM11 provide three of the data used: Global hemispheric flux up and down and Diffuse hemispheric flux down. Based on the first two, a surface shortwave budget (SWD/SWU=albedo) can be calculated. The diffuse measurements derive from CM11 being shielded from direct sunlight by a moving object, so that diffuse shortwave down + direct shortwave = Global shortwave. In the presence of clouds of sufficient optical depth diffuse shortwave = Global shortwave.

Kipp & Zonen CHP1 Pyrheilometer

The Kipp & Zonen CHP1 Pyrheilometer measures direct shortwave radiation. It utilizes the same principle as the pyranometer except it has a field of view of only 5°. It is mounted on a suntracker that pivots it around so that it stays directed at the sun at all times while it is up.

This instrument has a surface which is perpendicular to the sun. Using equation 4.1 gives its value in W/m^2 for a surface perpendicular to the sun, and so to get the flux recorded as W/m^2 for a plane surface, the output must be corrected with the local zenithangle. For UTC time, this can well be approximated by:

$$\cos\Theta = max(0, 23.45 * \sin(d - 80)\frac{2\pi}{366} + 11.05\cos(m + 764.2)\frac{2\pi}{1440})) \tag{4.2}$$

[1]Instruction Manual for CMA series. http://www.campbellsci.com/documents/manuals/kippzonen_manual_series.pdf

Where d is days since equinox in spring, offset to fit the Julian calendar, m is minutes since UTC midnight, corrected for local time and 11.05 is the angle from NYA to the North pole. A maximum of this value and zero is taken to avoid negative values.

$$E_{SW} = U_{emf}/S \cos\Theta \tag{4.3}$$

The CHP1 has the same thermophile and estimated error as the CH11, but an additional uncertainty must be taken into account due to the sun tracker. At high sun angles, and at times of variable cloud cover, the sun tracker uses some time to find the sun and will therefore not always be in the center of the instrument's view.

Eppley Pyrgeometer

The Eppley PIR pyrgeometer instruments measure longwave radiation. They have a similar design as the pyranometers, but with very different qualities. Also hemispheric, the silicone dome that protects the sensors from the elements also serves as a shelter for shortwave radiation. Relatively transient for longwave radiation ($4 - 50\mu m$), the thermophile is warmed exclusively by longwave radiation. The major difficulty is that the thermophile in the center of the instrument is greatly influenced by the instrument temperature Ji and Tsay (2000). Therefore, the temperature is logged in the instrument and recorded. For calculations two formulas are used[2]:

Simple formula:

$$Irradiation_{LW} = Ttp * C_1 + \sigma T_c^4 \tag{4.4}$$

Advanced formula:

$$Irradiation_{LW} = Ttp * C_1 + \sigma T_c^4 - 4\sigma(T_d^4 - T_c^4) \tag{4.5}$$

Ttp = PIR thermophile Voltage
T_c = PIR case temperature
T_d = PIR dome temperature
C_1 = PIR Calibration factor
σ= Stephan-Boltzman constant

The reason for having two different formulas is that previous to 2006 not all instruments had a dome temperature recorded, and therefore the advanced formula could not be used. This is a potential source of error. For the instruments in question, post 2006 difference has a mean square error (MSE)

[2]Application Note for Eppley PIR by: Campbell scientific, inc. http://www.campbellsci.com/documents/technical-papers/eply-pir.pdf

of about 2.3% when using simple versus advanced model, which is well above the instrument measurement error of only 1%. Percipitation and drift snow may also periodically influence measurements.

Pyrgeometers are used for both the upwelling and downwelling longwave hemispheric flux measurements. At the instrumentation rack they are about 90cm above the surface and the upward longwave flux may be used to represent surface skin temperature. The temporal resolution in the rawdata is 1 minute as for all the radiation measurements and the average value for this minute is what is used as input.

4.1.2 DMPS - CPC/DMA

The Differential Mobility Particle System (DMPS) is located within the station on Zeppelin mountain seen in figure 4.1 1). The elevated position it has from the settlement below ensures that it is relatively unaffected by it. This, combined with the fact that there are hundreds of kilometers to the nearest populated area, makes this an excellent site to measure background concentrations of aerosol. A research by Beine et. al. (1996) found that very special meteorological conditions had to be in place for the local pollution from Ny Aalesund to affect the measurements, and that this only happens 6.4% of the time.

The University of Stockholm run DMPS is used to observe the aerosol size distribution or concentration density as function of particle size. It consists of two main parts. A DMA (Differential Mobility Analyzer) to separate the particles according to their electrical mobility, and a Condensation Particle Counter (CPC) to count them. The DMA consists of a concentric cylinder arrangement with a center rod and an outer shell. The outer diameter is about 6 cm and the rod about 5 cm in diameter. The aerosol particles travel through the annulus in an otherwise particle free carrier air or sheath air.

The flow rate of the sheath air, which re-circulates via a so called closed-loop particle filter-pump setup, is 5-10 L/min and the sample air (aerosol stream) is 1 L/min. Between the center rod and the outer wall an electric field is established using a high voltage supply. Electrically charged particles can then move across the field while traveling the length of 28 cm. At the end of the 28 cm there is an opening or slit around the rod. For a given geometry of the DMA and a fixed voltage, only a very narrow range of particle sizes can reach this outlet. Particles that are smaller will be drawn to the rod at shorter distance; while larger will not travel laterally far enough. The particles that make it through to the outlet, are counted using a CPC instrument.

Aerosol size bins

#	Size Range
Bin 1	[17.8 - 22.4] nm
Bin 2	[22.4 - 28.2] nm
Bin 3	[28.2 - 35.5] nm
Bin 4	[35.5 - 44.7] nm
Bin 5	[44.7 - 56.2] nm
Bin 6	[56.2 - 70.8] nm
Bin 7	[70.8 - 89.1] nm
Bin 8	[89.1 -112.2] nm
Bin 9	[112.2-141.1] nm
Bin 10	[141.3-177.8] nm
Bin 11	[177.8-223.9] nm
Bin 12	[223.9-281.8] nm
Bin 13	[281.8-353.8] nm
Bin 14	[354.8-446.7] nm
Bin 15	[446.7-562.3] nm
Bin 16	[562.3-707.9] nm
Small	[17.8 - 70.8] nm
Large	[70.8 -707.9] nm
All	[17.8 -707.9] nm

Table 4.1: Sizes range of aerosol in each bin and group.

By stepping the voltage from a few volts to more than 10000 V, the concentration of charged particles as function of their size (electrical mobility) can be determined. As there is a size dependent probability that a particle is neutral, positively or negatively charged, or have multiple charges, the measured density function needs to be inverted based on the assumption of a so called Boltzmann charge distribution function. To achieve this distribution a radioactive source (Ni-63) is used to neutralize the aerosol. First the measurements are performed by increasing the voltage (small to large particles), and then back again to low voltages. This up-and-down scan takes 20 minutes. It is assumed that the aerosol distribution change little over the 10 minutes it takes to scan from low to high voltage and vice versa. Hourly average data is used in this study. The instrument scans from 10 to 900 nm diameter, but smallest and the largest sizes are uncertain and therefore discarded in this study. In this work the size distribution is divided into the 16 logarithmically equidistant size classes of table 4.1.

The CPC instrument is a CPC TSI 3010 is used at Zeppelin (figure 4.3). Particles of only a few nm in diameter are too small to be detected using optical techniques. Therefore, the particles in the instrument are first exposed to a saturated environ of typically Butanol vapor (also I Isopropanol or water is used in commercial instruments). The sample air is then cooled

down (in the condenser part) to generate a supersaturated environment. The particles quickly grow by condensation from a few nm to several μm in diameter. These sizes are readily detected by scattered light from a laser beam. Depending on the details of the CPC, instruments typically detects particles that are originally larger than 3 to 10 nm in diameter. The response time of the instrument is on the order of seconds, but typically one hour averages is used for analyzing data.

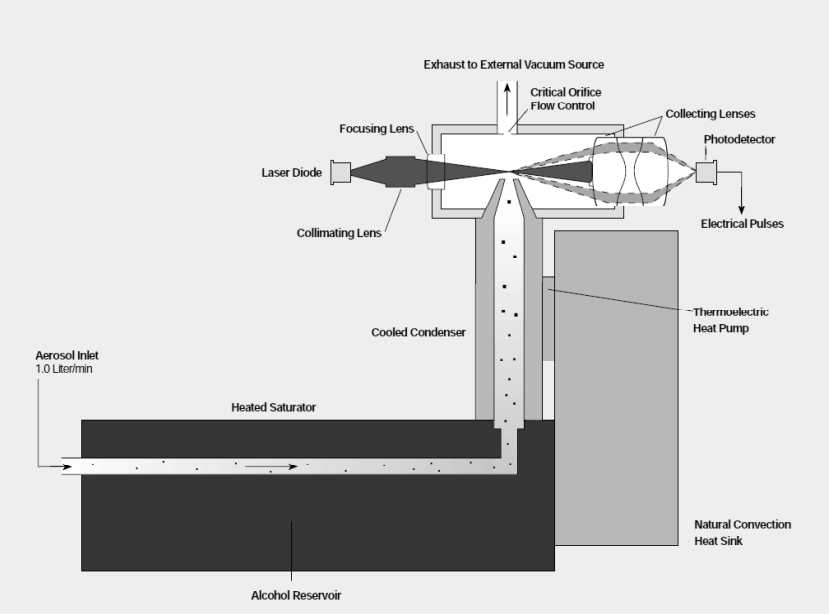

Figure 4.3: Schematic of how the CPC-3010 operates. Adapted from (Caldow et al 1992). The particular unit at Zeppelin uses butanol to saturate air.

4.1.3 Micropulse Lidar

The Micropulse Lidar (MPL) in NYA is part of a global atmospheric measurement system, namely the MPLNET. It was installed in 1998 and has since been in operation. For the first few years the MPL was directed at an angle to measure objects near the surface. Since May 2002, however, the MPL has been directed directly upwards and the data is now stored at NASA. The MPL is found inside the AWI building (figure 4.1) and operates through a window.

The SESI model MPL is a one-channel lidar[3] emitting at $\lambda = 523nm$. Pulses of polarized light beams are transmitted into the atmosphere, and the energy scattered back to the transceiver is collected and measured as a time-resolved signal.

[3]LIght Detection And Ranging (Lidar)

The backscatter signal received from a vertical directed lidar can be written (Ellingsworth et al., 2000):

$$S_r(z) = CE(\beta_R(z) + \beta_A(z))exp^{(\frac{-2}{R_R}\int_{z_L}^{z}\beta_R(z')dz')}exp^{(\frac{-2}{R_A}\int_{z_L}^{z}\beta_A(z')dz')} \quad (4.6)$$

$S_r(z)$ is the range corrected lidar signal. E is the emitted energy in the pulse and C the optical instrument constant. $\beta(z)$ is the unknown backscatter coefficient, R(z) is the backscatter-extinction ratio the equation must be solved for at each altitude z and z_L is the altitude of the lidar. The subscripts A and R denote aerosol and Rayleigh optical properties. To obtain results, an inverse lidar algorithm must be applied to the observed range corrected lidar signal (Ellingsworth et al., 2000).

The algorithm for cloud recognition used on the MPL in NYA is an adapted version for Arctic conditions by Masanori Yabuki of the original algorithm by (Ellingsworth et al., 2000; Campbell et al., 2008) for one channel lidar measurements. This algorithm defines backscatter above a given threshold as clouds. It gives the cloud base height and cloud top for up to 18 layers of clouds. It also gives a value for the furthest backscattered signal received, denoted as beamblock. In the presence of fog or precipitation, the lidar is blocked below the cloudbase.

The MPL has a vertical resolution of 30 m and under clear sky conditions it can observe backscatter from up to 14-15km. In the presence of clouds this would be significantly lower. For a cloud in the mid troposphere the extinction for the lidar would be roughly $LWP = 40g/m^2$. This is dependent on cloud height, temperature, the air below the cloud, as well as on cloud ice and ambient shortwave (Campbell et al., 2008).

The data output contains information on the position of cloud bases (in meters) with up to 12 possible layer. When possible, the vertical cloud top location (in meters) is included, as well as the highest altitude of backscatter signal received (beamblock). It is also possible to deduce information on the height of the planetary boundary layer (PBL) from this algorithm. The temporal resolution is 1minute and this average value is what is used as data.

4.2 Limitations

There are limitations in the instruments available at NYA, as well as in data availability. Before presenting the methods used to obtain the results it is therefore important to examine these limitations. Firstly, limitations in instrument measurements will be presented. Secondly, the process of combining data from the different instruments will be described.

Aerosols affect clouds by altering their microstructure. Therefore, to investigate the radiative effect changes in aerosols have on clouds, three essential

classes of observations are needed. 1) Radiative fluxes, 2) Aerosol properties, and 3) Cloud properties. As described above, the instruments at NYA fulfill none of these completely, combined, however, the instruments provide some information on all three classes of observations. The accuracy of results that can be obtained are determined by the quality of observations made. In addition, the number of parameters that are observed determine the assortment of results.The dataset used in this thesis is therefore compiled of several different measures from the instruments described above (section 4.1) which all need to be combined in order to obtain good quality results. In this section a detailed discussion about the limitations and possibilities of the NYA set of data follows.

The **radiation measurements** used are ground based and are hemispheric fluxes from the instruments listed in section 4.1. These measurements combine all radiation within their sensitivity range to calculate the total flux density. For many purposes this type of measurement is sufficient, but for more detailed investigations it has some shortcomings.

In order to perform more detailed investigations it a longwave radiation measurement with higher spectral resolution would be preferable, to examine in detail wavelengths where cloud emissivity is sensitive. This makes it possible to isolate cloud emissivity effects from other disturbances (e.g. Lubin and Vogelmann (2006)). An instrument that makes this possible is the Atmospheric Emitted Radiance Interferometer (AERI) which gives better than 1 wave number spectral resolution in the longwave. This instrument also makes it possible to retrieve vertical temperature profiles from the atmosphere (Feltz et al., 1998).

Although there is no AERI instrument at NYA, the reliability of the available pyrgeometer instruments are well documented and tested (e.g Ji and Tsay (2000)). The accuracy, on the other hand, is lower than desired in that the bulk spectral resolution of the pyrheilometer $285 - 2800nm$ and the pyrgeometer $4 - 50\mu m$.

Since the **aerosol measurements** at NYA are limited to the altitude of the inlet of air of the DMPS, it does not necessarily describe the vertical distribution of the aerosols so well. This is the a weakness in using a DMPS alone. It does, however, give accurate information regarding the size of particles, which many other retrieval techniques lack. If the DMPS was supplemented by lidar measurements, the total aerosol column could be estimated.

Correlation between accumulation mode aerosol and CCN is generally found to be very high (e.g Arctic study by Mauritsen et al. (2011)). Thus, measuring aerosols with the DMPS is very reliable within the mass of air it represents.

There are no observations of **cloud microsotructure** at NYA. This is a major obstacle when investigating cloud emissivity. The MPL is a one channel lidar, so it has only one pulse wavelength ($\lambda = 523nm$). From the backscattered signal the algorithm presented by Campbell et al. (2008) (and the revised Arctic version) interprets merely the strength of the signal, and gives cloud layer base and top from this.

More elaborate algorithms exist for more advanced MPL. If the receiving end of the MPL is able to distinguish the polarization ratio of the backscattered signal, or a more than one channel lidar is used, more information could be gathered. Based on the optical properties of aerosol at different wavelengths, and differences in backscatter polarization from water droplets and ice, many aspects can be determined. It is possible to retrieve total aerosol column and distribution, and cloud water phase and path. (e.g. Nishizawa et al. (2008))

A millimeter wave radar (RAdio Detection And Ranging) can observe cloud droplet spectra and the phase of water. Together with a multichannel polarized lidar it provides accurate information on all cloud properties (Clothiaux et al. (2000)). In determining cloud properties the data available from the MPL is unsuccessful. In comparison with other studies (Garrett and Zhao, 2006; Lubin and Vogelmann, 2006) very little is known about the clouds above NYA. There is one advantage with the set of data from NYA, and that is that the aerosols is measured at an higher altitude, so that it is more reliable that the mass of air in the cloud share properties with the aerosol sample.

Constructing a set of data

Combining the data from NYA research base gives a good, albeit broad, perception of the radiation and clouds. The lack of detail, however, is in part rectified by having very long time series and using statistical methods. A detailed explanation of the statistical methods used is described below (section 4.3) and statistical theory is included in Appendix A.

In order to account for the gap between the information provided by the instruments used and the desired information from the data they provide, a statistical approach was applied. When drawing sufficiently many samples from a distribution, the drawn samples will, with increasing certainty as samples increase, become representative the original distribution. By varying one property at a time while selecting data, variability due to a given property may be investigated and quantified. The following describes how the data was combined, and what methods were used to do this.

Radiation measurements dating back to 1974 were available, while before 1990 measurements were only available as hour-average values. Since then, minute average values are obtainable. In March 2001 an extensive refitting

of equipment was initialized at NP and instruments relocated, so there is a discontinuity to the measurements during that period. At AWI the radiation measurements are continuous since before 2000.

In May 2002 the MPL was relocated from its original placement. Initially set at a 30° angle it was placed and ready to operate at its current location at 15'th of May 2002. It is now directed vertically. Masanori Yabuki algorithm is not appliable to the angular measurement, so no data prior to its replacement have been included.

The DMPS located on Zeppelin has been operational since February 2000. It has periods where data is lacking, which seems to coincide with extreme cold conditions during winter. As is also the case for many of the other instruments. Fewer data is available for December through February. The primary datasets constructed from these measurements have three different purposes:

1. A set of data of minute average values spanning the period of the shortest available measurement (MPL) spanning 15'th May 2002-1'st of Nov 2010. This includes all measurements available, aerosol[4], radiation and MPL.

2. A combined set of data of aerosol and radiation for January 2000 - December 2010.

3. Hour averaged combined set of data for January 2000 - December 2010. This set of data has all available information on: aerosol, radiation, MPL[5] and meteorological observations of wind strength, wind direction, relative humidity (RH), specific humidity, pressure, temperature T and dew point temperature (T_d).

Dataset 1) includes only times where all instruments have a valid observation. Due to the large amount of data available, this is the smallest combination of data which is still accurate. The reason for having this set is to speed up computation. Dataset 2) has the purpose of investigating long term trends and statistical properties of aerosol and radiation, that would otherwise be influenced by including odd seasons. Dataset 3) combines all available information on hour average. Times of no measurements are treated as data missing.

All the longwave radiation used are those of AWI while global shortwave belong to NP instruments. The reason for this is that longwave radiation

[4]hour average used for every minute of the hour

[5]The algorithm for hour average cloud observations by the MPL include a cloud fraction parameter that states the fraction of the hour the MPL actually observed clouds and the variance of the height of the lowest cloud base as well as mean values for the hour.

measurements from NP had some shortcomings in documentation. From the pyrheilometers and pyranometers used for shortwave measurements NP data was selected due to the possibility of combining more than one instrument reading.

Because of the state of most of the rawdata available a thorough explanation on going from rawdata to usable data have been presented here. The datasets constructed as described above should make it possible to perform investigations in order to test the research questions. It is not made a point of distinguishing between the three dataset, they are used when appropriate.

4.3 Methods

Based on established theory and previous methods (chapter 2 & 3), the hypothesis is: **When many accumulation mode aerosols are present on Zeppelin mountain, a cloud formed in the vicinity will have lower r_e than if few accumulation mode aerosols were present. If the cloud formed has emissivity lower than unity, having a smaller r_e increases cloud emissivity and therefore cloud longwave forcing will increase.** The procedure constructed to test this hypothesis has 4 major components:

1. Separate instances of high and low accumulation mode aerosols number count.
2. Identify sensitive clouds.
3. Quantify radiative differences.
4. Validate results obtained.

In the following section each of these steps is discussed further.

4.3.1 Cloud droplet approximations

All data in its final form has a minute average basis, with the exception of aerosol data, that due to a long cycle to collect, were only available on one-hour averages. Based on this, the hour averaged aerosol data were taken as valid for every minute of that hour. The alternative to this would be to interpolate the aerosol measurements between the hourly values. The aerosol counter at Zeppelin mountain is some distance (1200m from figure 4.1) from the other instruments at the base in NYA, but using hour average should make it so that this distance is negligible.

Taking a mean value instead of interpolating makes very little difference since the hourly correlation from one hour to the next is 0.96. The distance

between the two observational sites also does not necessarily mean that a forward interpolation is more accurate.

The 16 aerosol bins from table 4.1 were divided into two sizebins, The large 70-500nm bin corresponds to the accumulation mode aerosols, and the small 10-70nm bin to the Aitken mode aerosols. Of the two, the accumulation mode is of particular interest. The accumulation mode particles are the ones that primarily act as CCN, depending somewhat on the hydoscopicity the larger an aerosol is, the lower supersaturation is needed for activation.

Previous investigation (Beine et al., 1996) indicates that clouds in this area should be a source of small aerosol particles, especially during winter, and that clouds tend to be a sink for the larger particles. The estimate from previous research indicated that the rough border for depletion and production for aerosols were around 70nm (J. Ström private com.). That the accumulation mode is not locally produced ensures that aerosols are well mixed. This further reinforces the assumption that the distance of the DMPS to the other instruments is negligible.

The aerosol measurements at Zeppelin at an altitude of 474m can be seen as a measurement of aerosol density under a cloud; if that cloud is near enough above Zeppelin and therefore is influential to the concentrations of aerosols the cloud was formed on.

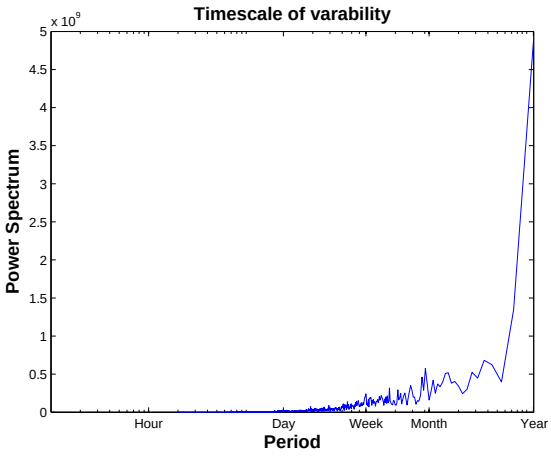

Figure 4.4: Fourier transform power spectra of accumulation mode aerosols plotted against the period. It is dominated by low frequency ($period^{-1}$) variability with the strongest signal the year long period of seasonal variations. Also distinguished is the lunar cycle $\sim$ 28 days and half of that cycle.

From the ranked aerosol number concentrations, high and low percentiles were constructed. These percentiles contain some percentage of the highest

and lowest number of accumulation mode aerosol observations from dataset 1). For simplicity, the high aerosol percentile is denoted as polluted and the low aerosol quartile clean.

A strong seasonal cycle was detected for the total aerosol number count as depicted in figure 4.4. Due to this, in order to get a comparable cloud sample with both high and low accumulation mode aerosol number concentrations, the aerosol count was divided into monthly groups and percentiles were selected from each month. Using these monthly percentiles ensures that both percentiles include observations that are spread roughly evenly throughout the year. Without doing this, there would be a bias for the accumulation mode aerosol rich months to be over-represented in the polluted dataset.

The loss from using the monthly percentiles is that there were instances with higher/lower accumulation aerosol count that was ignored. It was found that the former procedure largely outweighs the latter because of the strong influence of temperature on radiative fluxes. Due to temperature differences, seasons are not intercomparable. Because of this it is important to have an equal number of estimations from all seasons.

Of percentiles used, the results of grouped monthly quartiles[6] are given most attention. Some results of fewest and highest halves using the same approach as above are also presented.

4.3.2 Cloud location & properties

Clouds of interest were clouds with low LWP, so that changes in r_e changes emissivity. As seen in figure 2.4not all clouds are equally sensitive to droplet spectra changes. Since no instrument measure other cloud properties, limiting the clouds by their LWP is the only option to ensure that sensitive clouds are selected.

The ability of the MPL to detect exact optical thickness of a cloud is limited to detecting vertical thickness of the cloud, if the cloud is optically thin enough for the MPL to recieve backscatter from above the cloud. The limit for MPL's of similar capacity to the one i NYA have been found to be about $LWP = 40g/m^2$ (Campbell et al., 2008). When a cloud gets more liquid water than that, in general it becomes too optically thick for the MPL beam, and nothing above it is accurately measured. In accordance with this, when clouds above NYA were too optically thick for the MPL to penetrate, no recording of cloud tops or anything above were made, which indicate they are on average less sensitive (figure 2.4).

[6]The high quartile being the 25% with the most accumulation mode aerosol and the lower quartile the 25% with the fewest, drawn from each month and grouped.

From the approximate threshold value of the MPL's ability to penetrate dense clouds, two categories of clouds can be separated: 'thin' and 'thick' clouds. Thin clouds are where the MPL is able distinguish a cloud top. Thick clouds are where the beam is made extinct within the cloud and no cloud top is recorded. The dominating feature that placed clouds in one or another category is cloud LWP. Clouds with a recorded cloud top are denoted as 'thin' clouds and clouds without a recorded cloud top are denoted as 'thick'. Thin clouds have a low LWP and therefore are the most sensitive.

Clouds of interest are water or mixed phase clouds.These are particularly abundant in the lower troposphere in the arctic during the summer. Following previous research (Lubin and Vogelmann, 2006) it is probable that the majority of clouds that have a base at 2km or lower will be water or mixed phase clouds. Based on this, a limit for the highest cloud base was set at 2km. Also, to ensure that the aerosol sample was under the cloud the lowest CB was set at 600m. In a recent paper by Devasthale et al. (2011) satellite observations substantiate the claim that low stratiform clouds are predominately liquid, even with cloud temperatures down to $-30°$.

By limiting the cloud base to altitudes close to that of the aerosol measurements, it is ensured that observed aerosols are similar to the aerosol levels present when the cloud formed. Filtering the observations by these standards provide clouds of low LWP's. Due to the limitations of the altitude of the cloud base, the probability that the clouds are liquid is maximized. This also ensures that the aerosol measurements are valid for the cloud, so that separating aerosol counts lead to different r_e.

4.4 One dimensional model

A one-dimensional column model suited to estimate instantaneous fluxes signify the same parameters as ground observations and is therefore an excellent tool. Intercomparison between model and observations is therefore of great value, since the model then can provide additional information.

In this thesis, the model used for this purpose is a modified version the 1-D radiative code of NCAR CCM3 (Alteskjær et al., 2010). It was first built by J.E. Kristjánsson and G. Myhre at MetOs and modified again by K. Alteskjær. The model was run with 26 layers and it is designed to give instantaneous radiation fluxes. User options such as cloud layer, cloud fraction, LWP and ice fraction, makes it a versatile tool for studying cloud forcing. The output values are latitudinal 24 hour averages, which is important to note for shortwave results. The parametrization in the model of β_{abs} and Q_{abs} are the empirical values calculated by Garrett et al. (2002).

Standard atmospheric profiles for the Arctic for both summer and winter, as well as autumn was added to the model by Alteskjær et al. (2010). The model allows for numerous options such as cloud LWP, r_e, CVT and more. This makes it an agile tool to investigate different clouds of varying properties. Section 4.3.1 shows that much of cloud microstructure is unobserved, and using this model provides some insight into that issue. By replicating the known features of the clouds observed, the remaining attributes may be indicated by the model values. The model may thereby provide additional information on cloud microstructure. This allows for a theoretical evaluation of the observed measures.

This chapter has presented the instruments used to obtain the dataset for this thesis, as well as the methods used to examine it. Measurements from NP, AWI, NASA and SU provided a raw dataset which has been statistically, methodically and manually sorted to provide usable data (section 4.2). Limitations in the instruments available, as well as in the raw data have been presented (section 4.1). Statistical methods were used to account for missing data due to data resolution and most of the statistical methods used are presented in (appendix A). How clouds and aerosol regimes of interest have been presented in sections (4.3.2 and 4.3.1), as well as the 1-D characteristics of the 1-D model (section 4.4). It is based on the methods described above that the results in the following section were obtained.

Chapter 5

Results & Discussion

The following chapter presents the results derived from collaboration of the data presented in the previous chapter. Following this, a discussion of the findings will be provided. With the 11 year long series of measurements, many atmospheric properties may change over time. Therefore the climatological factors most related to clouds have been investigated and are presented in the first part of this chapter (5.1 and 5.2). These observed atmospheric properties may have important implications for the investigation of the cloud emissivity effect next presented.

In section 5.3, 'Increased surface longwave forcing', the results obtained by using the method of sections 4.3.1 & 4.3.2 are presented. Within these results, a number of features are presented and then discussed, along with the implemented model results. Finally, a validation of the metods used is presented (5.4), with the aim of justifying that the observed $\Delta SLWCF$ is due to an increased cloud emissivity.

5.1 Ny Aalesund climatology

Temperatures

The 2m temperature measurements show that the mean observed temperature in NYA is $-4.6°C$ increasing in trend from $-5.2°C$ in 2000 to a predicted temperature of $-3.6°C$ in 2011 (figure 5.1). It is a significant trend of warming and above predictions made by IPCC (2007) for the Arctic.

The longwave flux trends in figure 5.1 are those of AWI. The trends of 1.429 $W/(m^2yr)$ and 1.435 $W/(m^2yr)$ for LWU and LWD are both significant, coherent with the observed warming of the 2m temperature. A notable feature of the upwelling radiation is the steady maximum that dominates for much of the year at about 315 W/m^2. This is, using Stefan-Boltzmann's law (eq. 2.2), equivalent to surface skin temperature very close to $0°C$, and is due to snowmelt. Before all the snow at the surface is melted, surface skin temperature will not rise above this level and for as long as the snowmelt continues the LWU will not increase noticeably.

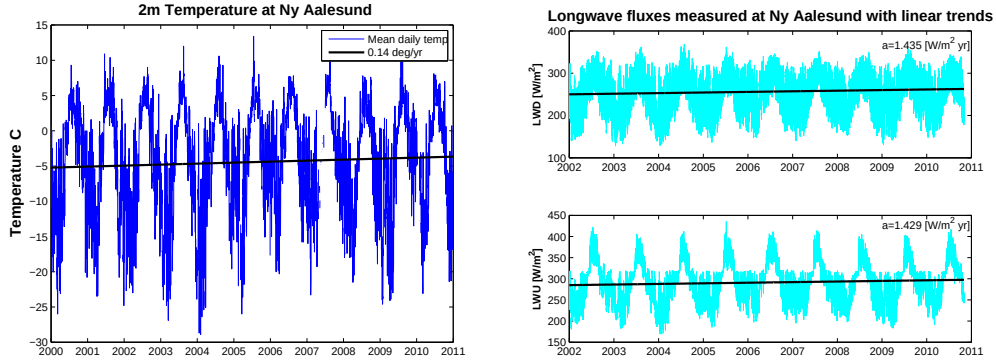

Figure 5.1: Temperature and radiation showing similar trends. Temperatures shown are 24h average values from dataset 3 (left). Longwave hemispheric fluxes with linear trends from dataset 2 (right). The LWU (bottom) shows a significant trend consistent with a surface warming. LWD (top) has a similar trend, the reason for this may have a more complex explanation.

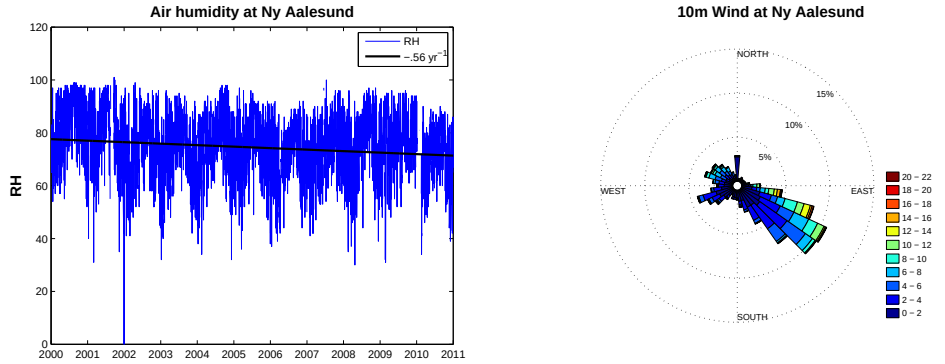

Figure 5.2: Left: Airhumidity based on 24h average values from dataset 3. The sinking trend is significant. Right: Wind rose showing dominant wind direction and strength. The dominant SE wind is roughly aligned with the fjord. Wind strength (in m/s) have individual colours.

Wind and Humidity

The wind is dominated (64%) by winds from between east and south (figure 5.2). This is a wind along the fjord towards open sea. NYA is protected from strong winds from the SW and NE by mountains with peaks above 500m. Relative airhumidity shows a significant trend to decrease (figure 5.2). The relative humidity is important because altered relative humidity should influence cloud formation. Specific humidity (not shown) has no significant trend. This points to the warming temperature as a cause of the falling RH, since water vapor content in the air is close to constant.

Depending on the year, the fjord is frozen from around November to March. If ice formation on the fjord is set back by the warming trend, this should allow for a stronger flux of water vapor from the sea into the atmosphere around NYA. There are, however, many things influencing atmospheric water vapor along with airtemperature like surface moisture and temperature, sea temperature, turbulent mixing from winds. The important implication of the airhumidity is that water vapor itself as a greenhouse gas has no detectable trend, but that the trend in RH may influence cloud base height and LWC of clouds (Curry et al., 1996).

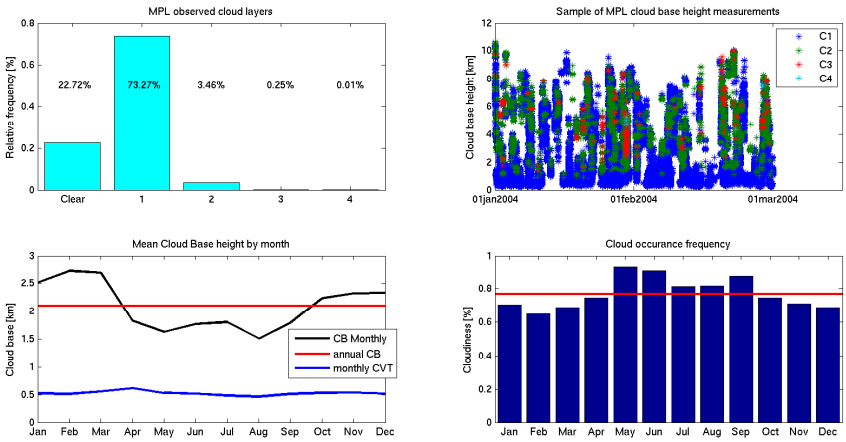

Figure 5.3: Some characteristics of the clouds observed by the AWI MPL over Ny Aalesund in the timeperiod May 2002- Nov 2010. Top left: a) Annual mean cloud layers. Top right: b) Clouds found by the MPL for a short timeinterval. CB1 is the lowest cloud base found, CB2 the second lowest etc. Bottom left: c) Annual and monthly average cloud base height. CVT referrs to cloud vertical thickness. Bottom right: d) Relative frequency of observed clouds. Red line is the annual average.

Cloudcover

Cloud characteristics are measured by the MPL and are measured during the period May 2002- Nov 2010 (figure 5.3). The mean annual cloudcover was found to be 77%. This cloud cover is roughly what has been measured elswhere in the Arctic (e.g. Devasthale et al. (2011); Initieri et al. (2002b); Curry et al. (1996)).

Observations in NYA show slightly lower seasonal variability than Devasthale (2011) finds for the region $66 - 80°N$, and a somewhat lower annual average than those measured by the SHEBA campaign (Initieri et al., 2002b). Most interestingly results obtained at Barrow (Curry et al. (1996), T. Garrett

private com.) show similar cloud frequencies above Barrow. Thin low level stratiform clouds at the two places should have roughly the same frequency.

The mean number of cloud layers was measured to 1.05 when there are clouds present, but is likely to be much higher. A ground based lidar beam gets extinct in dense clouds and if the lowest cloud is dense, any cloud above is not observed.(Devasthale et al., 2011). Initieri et al. (2002b) used a ground based lidar in the Beufort sea for measurements of cloudlayer data, in order to discover that the winter is typically single layered and the summer is multilayered. The combination of lidar and millimeter radar make detection more efficient, and allow for observations of thinner cloud layers than what is possible with only an MPL. Overall they detected multilayer clouds much more frequently than what is observed above NYA. This may reflect a difference in cloud structure, as the two places are far apart, but may also reflect the superior detection technique of combination with millimeter radar.

The mean cloud base height (CBH) was found to be 2140m at NYA with a long tailed distribution where the lowest clouds were more common. The observed vertical thickness only includes clouds of an optical thickness less than the MPL extinction limit of about $40g/m^2$. It is valid for clouds less optical deep than this as well, but is probably not a good estimate for over all average vertical thickness for clouds with greater LWP than this. There is a clear seasonal dependence for the monthly average CBH. It is higher in the cold months than in the warm months. This is consistent with observed seasonal variations in RH (figure 5.2). Air of high RH in summer have a lower lifting cloud condensation level than cold dry winter air.

5.2 Aerosol properties

Data from the DMPS are represented in figure 5.4 and 5.5. Among some interesting features they display, are the correlation between the large and small sizebin, which is low: only 0.28. The correlation between aerosols close in size is strong, but reduces with an increasing difference in size. This has large implications for what aerosol sizes should be included as CCN, as the larger aerosols are the most efficient CCN and will be activated at lower supersaturation. If aerosols of sizes which are so small that they would never be activated were to be counted as CCN, they would influence results. Since the smaller Aitken mode and larger accumulation mode aerosols are so weakly correlated and, especially during summer, the smaller dominate in numbers, including these aerosol would have lead to a weaker correlation between CDNC and aerosol number.

As figure 5.4 c) & d) show, there are two distinct aerosol regimes dominating. The larger aerosols that dominate in the dark and intermediate months are

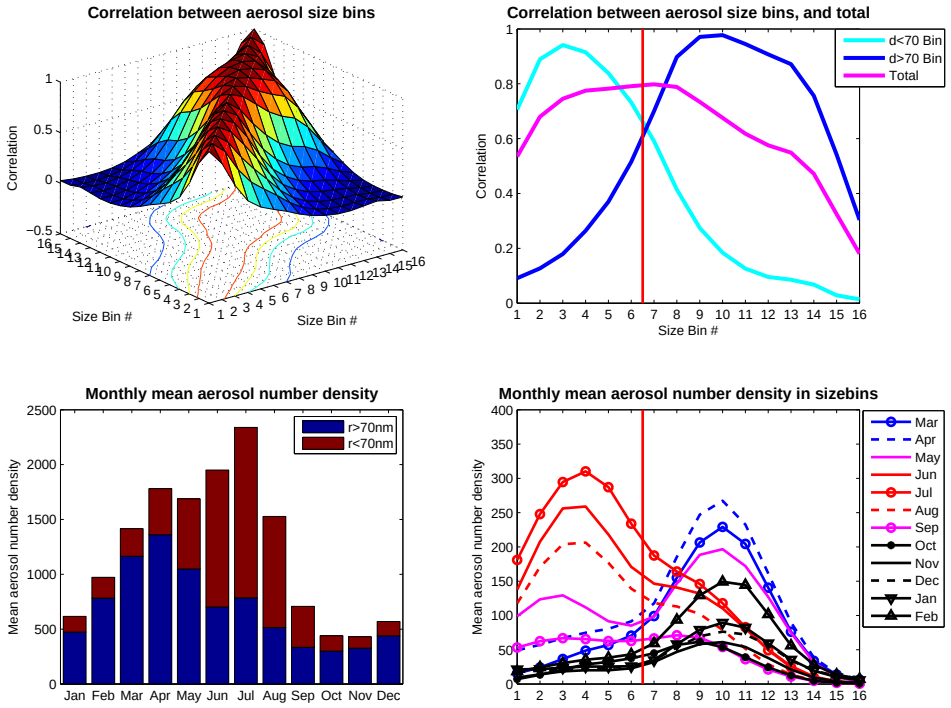

Figure 5.4: Characteristics of the aerosol numbers observed in the period 2000-2010. Top left: a) Correlation between all aerosol size bins. Top right: b) Correlation of the accumulation mode (d>70nm) and Aitken mode (d<70nm) aerosols and the total aerosol number density. Bottom left: c) Total aerosol density numbers per month divided in large and small aerosols. Bottom right: d) Monthly aerosol numbers. Red lines are summer months with midnightsun, blue and purple lines are intermediate months while black is dark months. Note the two distinctly different modes. Vertical red line is the 70nm division between small and large aerosol.

very likely primarily transported aerosols from lower latitudes. The small aerosols that dominates in summer is locally produced aerosol that are dependent on shortwave radiation to form (Martin et al., 2011). The notably stronger trend in the accumulation mode aerosols are possibly due to emission reductions in North America and Europe, and will be discussed in section 5.4.2

5.3 Increased surface longwave forcing

In this section the results of the primary objective of this thesis, which is to examine if there is a measurable surface indirect longwave forcing, are presen-

ted. Following the methods presented in section 4.3, using upper (polluted) and lower (clean) quartile aerosol number densities and the low clouds that are also thin, leaves 10346 and 10142 minute long observations respectively. Using this procedure should differentiate clouds with high CDNC (polluted) and low CDNC (clean). Section 2.2 shows that increasing CDNC, increases emissivity (ϵ) of clouds that have ϵ lower than unity (i.e. clouds of low LWP). An increase in cloud longwave emissivity in terms of observations at the surface, can be described by the equation 2.8:

$$\Delta SLCF = F^{LW}_{polluted}\downarrow - F^{LW}_{polluted}\uparrow - (F^{LW}_{clean}\downarrow - F^{LW}_{clean}\uparrow) \quad [W/m^2]$$

The equation 5.1 shows the observed mean values of the pyrgeometers of AWI in the presence of thin low clouds in the period between January 1st 2000 and December 31st 2010:

$$\Delta SLCF = 256.57 - 300.93 - (254.58 - 302.51) \quad [W/m^2]$$

$$\Delta SLCF = 3.57 \quad [3.21 - 4.87] \quad [W/m^2] \tag{5.1}$$

[3.21-4.87] in equation 5.1 is the 95% confidence interval established by the Kolomogorov-Smirnov (K-S) statistics (described in Appendix A) based on the sample sizes of the 10346 polluted and 10142 clean observations. A two-sided K-S statistics test of the two datasets, set against a normal distribution of equal mean and variance, showed that there was a probability of above 99.9% that the samples were not from a normal distribution; thereby rendering normal distribution based z- and t- statistics tests, unsuitable. A K-S statistics one-sided test for difference in mean was therefore chosen as

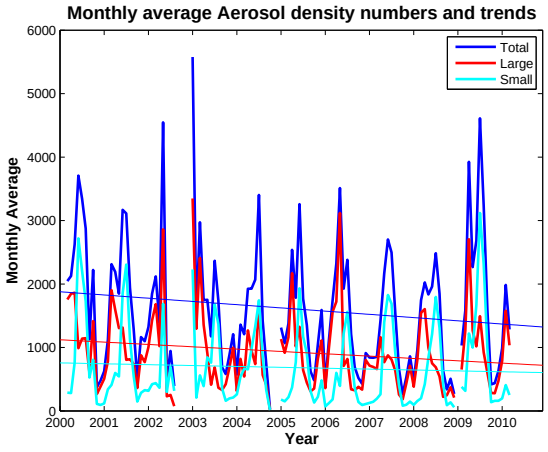

Figure 5.5: 2000-2010 Aerosol trends show a significant trend for a decrease in total aerosol number of $-48.3N/(cm^3yr)$. The decrease is largest for aerosol 70-500nm with $-41N/(cm^3yr)$, but also small aerosols show a weak (but not significant) trend to decrease.

it utilizes empirical cumulative distribution functions (ECDF) that are not dependent on any distribution. A plot of the two ECDF's for the clean and polluted clouds is shown in figure 5.6. This shows the difference in surface longwave forcing between the polluted and the clean clouds.

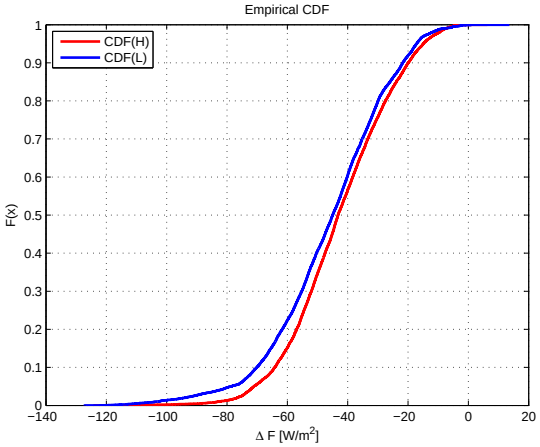

Figure 5.6: ECDF for F_{net}^{LW} of the polluted (Red) and clean (Blue) quartile aerosol of thin low clouds. ΔF is the net surface longwave heatingrate. For the entire year, a K-S test results in the maximum likelihood for the difference in mean to be 3.57 W/m^2 for unpaired samples.

A slight surface temperature difference was observed between the clean and polluted clouds. The mean downwelling pyrgeometer flux difference was slightly higher for the clean than the polluted clouds, 2.01 W/m^2, showing that the surface was slightly warmer at the times of the clean measurements.

Establishing that there is an increase in surface longwave cloud forcing from the clean to the polluted clouds does not necessarily mean that this increase is due to a cloud emissivity effect. There are many properties of clouds that affect cloud surface forcing, and sections 5.4 & 5.4.1 adress these properties, arguing that what is observed is in fact a cloud emissivity effect.

As it is not obvious that the algorithm of section 4.3 is the only way to measure a cloud emissivity effect, the next section contains some variations of this method, both in terms of what aerosol limitations were used and in terms of what clouds to include. Also included here is an investigation on the frequency of clouds that are included.

Results from different limiting criteria

Looking only at the percentiles at the extremities should produce the clouds of most different CDNC, however, this does not necessarily include all clouds

that can be affected. Also, figure 2.4 shows that there are sensitive clouds that have a $LWP > 40g/m^2$, which is the estimate for the MPL thin cloud. The following section presents some other limitation criteria used for aerosol and cloud thickness.

As with aerosols, a number of different percentiles was applied to look in detail at what conditions changed the surface cloud forcing. Most interesting is the 50% percentile which is all the data with higher than median aerosol number measurements in one bin, and the rest in the lower bin, giving a forcing of 1.54 W/m^2 with 95% confidence [1.04 2.03].

This result is based on 23440 and 27953 minute observations for polluted and clean aerosol respectively. These numbers show that there is only a very weak (but not significant at 75% statistical confidence) measurable increase in surface longwave cloud forcing of the middle data[1], ranked by aerosol concentrations (25-75%).

Using the ranked halves of the aerosol distribution, there is only a very weak signal between aerosol group 25-50 & 50-75 %. Subtracting the effect of the end quartiles (0-25% and 75-100%), gives a 95% confidence interval of [−0.07 0.31] W/m^2 for the center of the aerosol distribution. From this it is not obvious that a small increase in aerosol numbers at instances where there are already many will have an effect. By this it should be noted that the results obtained are sensitive to what percentiles are used.

Limiting the clouds so that they are thin enough, so that the MPL can observe the cloud top, has many advantages. However, it also has the disadvantage that there are much fewer observations to rely on. By not limiting to thin clouds, there are about 20 times as many observations. Still, with a low cloud base, the number of minute observations increases to 256,078 & 236,599 for the polluted and clean respectively. These clouds show a significant difference in surface forcing of 1.74 W/m^2 with a 95% K-S confidence interval at $[1.59 - 1.89]$.

5.3.1 Annual estimates

One of the most important differences between observational results (Lubin and Vogelmann, 2006; Garrett and Zhao, 2006) and modeled results (Alteskjær et al., 2010) thus far has been that observed results have described a local instantaneous forcing for selected clouds, while modeled results have been pan-Arctic annual results. An observational annual estimate may therefore provide some insight to the difference of these results. By

[1] Comparison between the 25-50% and 50-75% highest accumulation mode aerosol number concentration data

Summarized Results

Type of clouds	Frequency	Aerosol	95% CI	Potential
Low thin clouds	0.90 %	$25pct^2$	$[3.21\ 4.87]^1$	$[0.031\ 0.045]^1$
Low thin clouds	2.54 %	$50pct^3$	$[1.04\ 2.03]^1$	$[0.026\ 0.052]^1$
Low clouds	15.40 %	$25pct^2$	$[1.59\ 1.89]^1$	$[0.240\ 0.290]^1$

Table 5.1: Low clouds are clouds with cloud base 500-2000m. Thin clouds are clouds which the MPL can see through. The confidence interval is based on K-S ECDF statistics. The frequencies are occurrences divided by total observations in dataset 1. Potential is the annual estimate of frequency multiplied by surface forcing. [1] W/m^2 [2] Quartile aerosol distribution 0-25% & 75-100 % [3] Higher and lower than median 0-50% & 50-100 % aerosol number concentrations.

analyzing cloud occurrence frequencies, this section aims to establish annual estimates for the observed increase in cloud forcing from increased CDNC.

Table 5.1 summarizes the results found by the different limiting criteria. Singling out the low clouds with low LWP (Low thin clouds) gives the strongest signal. These have the strongest difference in surface forcing when they occur, but are very infrequent above NYA. Allowing for higher LWP (Low clouds) gives a much weaker signal, but since these clouds are much more frequent, these are more important annually. The low thin clouds are included in this group, but account for only $\sim$ 6% of these clouds. This shows that the number of clouds affected is large, and extends well beyond the threshold value which the MPL can see through.

The annual estimate in table 5.1 is not an estimate of the actual forcing by cloud emissivity effect . It is an annual potential of the effect measured. If the clouds formed under low aerosol concentrations are representative of unpolluted Arctic air, and those formed under high aerosol concentrations are polluted instances, the value represents the warming if all clouds were polluted. If all the clouds in the upper quartile represent the polluted clouds that would otherwise be in the lower quartile, the forcing would be a quarter of the annual values in table 5.1. Alteskjær et al. (2010) did, however, find similarities between a preindustrial aerosol regime and Garrett and Zhao (2006) clean clouds, that may strengthen the validity of the estimates of table 5.1.

Seasonal estimates

A higher time resolution than annual might be desirable, because forcing may have different feedback mechanisms throughout the year. Therefore, seasonal estimates are provided. Autumn and summer have many observations, while winter has fewer, and spring has somewhere in between. Differences in the number of observations may be influenced by instrument up-time, which is

significantly lower in winter. Average up time is 67% for dataset 1, i.e. the times when all instrument have valid[2] and complete observations.

The percentages for the different seasons are for spring, summer, autumn and winter; 66 71 74 59 respectively. When allowing for seasonal differences in seasonal up-time the annual $\Delta SLCF$ is given by:

$$\Delta SLCF_{adj} = \frac{1}{N}\sum_{i=1}^{4} W_i^{up-time} \times n_i M_i \quad = 3.83 \quad [W/m^2] \qquad (5.2)$$

In equation 5.2, N is the total number of observations, n_i the number of observations in month i, $W_i^{up-time}$ is the instrument up time weighing function and M_i the observed $\Delta SLCF$ of month i. $\Delta SLCF_{adj}$ is thus the annual instrument up-time adjusted $\Delta SLCF$. The result of 3.83 $[W/m^2]$ is slightly above the annually produced estimate, because there are less observations during winter when the observed result is strong.

Figure 5.7 shows the seasonal distribution of the low thin clouds using aerosol quartile. Seasonal variations show a strong observed signal during winter and a negative to weak autumn signal. Summer and spring show a positive signal. The red bar is adjusted for the relative observed frequencies $\frac{n_i}{N}$ of 0.22 0.32 0.32 0.15 for spring, summer, autumn and winter respectively, and the instrument weighing function. An accurate estimate for the confidence interval could be obtained by eq A.11, but the unknown term of the LWU covariance between the seasons makes this calculation impossible. With an unknown certainty of this estimate, the annual result of 3.57 $[W/m^2]$ remains the best annual estimate.

To accredit the observed $\Delta SLCF$ between the clean and polluted air masses, as a cloud emissivity effect is based on the assumption that the only difference between the polluted and clean clouds, is the CDNC. This assumption will be elaborated on in section 5.4.1. In the following section 5.3.2, a study of the other possible effects of increased aerosol number concentrations will be presented.

5.3.2 Other Aerosol effects

From figure 1.1, it is obvious that the first longwave effect is not considered a major contributor to climate forcing on a global scale. The other aerosol effects are considered to be larger, and it is therefore important to see if it is possible to find these effects for the clouds investigated above NYA.

Alteskjær et al. (2010) found that the corresponding surface shortwave indirect effect to the modeled longwave of 0.10 to 0.85 W/m^2 was -1.29 to -0.52

[2]Accepted by the data filtering scheme of section 4.2

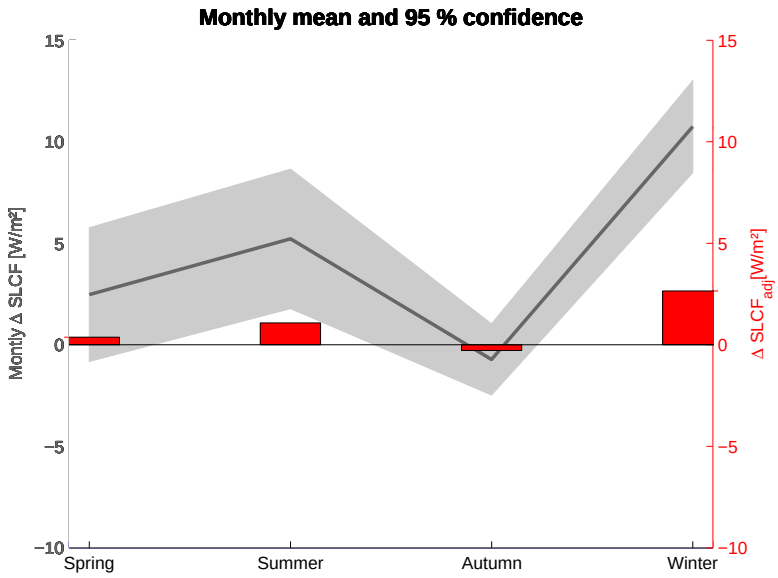

Figure 5.7: Gray: Longwave indirect forcing for the seasons with 95% confidence interval using quartile aerosol distributions. Red: Relative contribution to annual result weighted by eq 5.2, show the strong winter signal as the most important, even though there are fewest observations then. No specific explanation for the negative forcing in autumn has been uncovered, but these three Autumn months are very climatologically different and this may influence the variance.

W/m^2. The longwave effect was only found to be dominating during winter. Both Garrett and Zhao (2006) and Alteskjær et al. (2010) found an increase in LWP of 2.3 and 2.4 $[g/m^2]$ for the low to high quartile aerosol concentrations and preindustrial to present SO_4 respectively. This also indicates that there must be substantial cloud lifetime effects, which should also be investigated.

In order to obtain valuable results when using a statistical approach it is essential to have as many observations as possible. Obtaining strong observations of other aerosol effects from this set of data is limited by the limitations described in 4.2. Some additional limitations apply to shortwave radiation measurements.

The approach of section 4.3 should also be valid for investigating cloud albedo effects. There are, however, some additional considerations to be made. Shortwave radiation is only present during roughly half the year, and when present often from a sun low on the horizon. The highest elevation of the sun in NYA is at an 55.67° angle above the horizon. The average sun zenith angle is thus very high in NYA, and an unfortunate effect of this is the instrument

Number of Clouds Observed

Type of clouds	High Aerosol	Low Aerosol
Low thin clouds 25pct	10,346 (50.5%)	10,142
Low thin clouds 50pct	23,440 (45.6%)	27,953
Low clouds 25pct	256,078 (51.9%)	236,599

Table 5.2: The number of observations for each selection process used. For thin clouds the method does not necessarily imply that increased CDNC should lead to more high aerosol observations due to diverging implications of increased CDNC. For the low clouds more observations in the presence of many aerosol may indicate an increase in lifetime.

accuracy decreases (section 4.1).

Additional considerations include the surface albedo measured inaccuracy described in section 4.1 and the high frequency of clouds (figure 5.3). These additional uncertainties compared to longwave radiation, makes it harder to get an accurate surface shortwave radiation budget.

Since the pyrheilometer (section 4.1) follows the sun and the MPL measures clouds directly above, these instruments do not necessarily observe the same conditions. Investigations of data show that the variance and instrument uncertainties are an order of magnitude larger than the expected signals. Because of this, no dependable shortwave radiation results were obtained.

Lacking sufficiently accurate shortwave radiation information limits the ability to observe many other aerosol radiative impacts. Cloud lifetime effects of increased CDNC (figure 1.1) would be apparent by a difference in observed frequencies under the different aerosol regimes. An increase in cloud CDNC tends to increase cloud vertical extention, LWP and lifetime (figure 1.1). A longer lifetime of clouds with higher CDNC would lead to more observations of clouds with high aerosol number concentrations. An increased LWP would lead to fewer low thin clouds under high aerosol conditions, as would an increase in CDNC itself, due to the threshold optical depth value of the MPL. These effects work against each other, as table 5.2 suggests. The perhaps only suggestion of an increased lifetime is for the low clouds, when only the lifetime effect influences the clouds.

From the data of table 5.2 it is not possible to conclude on an observed lifetime effect. It is, however, plausible that a proportion of the measured annual estimate by the 'Low clouds' of table 5.1 and 5.2 is influenced by increased LWP. However, since LWP of clouds are among the unmeasured quantities at NYA, it is hard to conclude.

5.3.3 Model input

Model results are dependent on what cloud parameters and what season the model was run for. To get as accurate as possible model input it is therefore of vital importance that the modeled cloud is as similar as possible to the mean clouds on which the results are based. To get to this, an analysis of total cloud forcing was applied.

An estimate of total longwave cloud forcing at the surface was found by comparing the surface fluxes of the mean cloud, to the surface fluxes of that of a clear sky. Mean SLWCF of all clouds selected (both polluted and clean quartile), shows a 16.38 W/m^2 increased longwave forcing compared to annual clear sky average. The clear sky average was calculated by taking the mean fluxes of the clear sky observations described in section 5.1. Subsequentially, the following equation 2.8 was used :

$$SLWCF = F^{LW}_{cloud}\downarrow - F^{LW}_{cloud}\uparrow - (F^{LW}_{clear}\downarrow - F^{LW}_{clear}\uparrow) \quad [W/m^2]$$

with an annual mean difference in LWD flux of 69.12 W/m^2:

$$SCF^{LW} = F^{LW}_{cloud}\downarrow - F^{LW}_{clear}\downarrow \quad [W/m^2] \tag{5.3}$$

The large difference between surface forcing and LWD indicates a surface heating under the clouds, since the observations where clouds are present show a much higher LWU and thereby a higher temperature (eq 2.2). These results were then used to construct a cloud with as similar a forcing as possible to these clouds, in a model.

Since cloud microstructure parameters as r_e and LWP is unknown, a comparison with model results may give an indication of what the microstructure must be like to produce the results observed. The lack of cloud microstructure information in the data makes it hard to evaluate one cloud individually. Therefore, the cloud used to compare with the model is the mean cloud of clean and polluted.

Summarizing the quartile data set for the thin low clouds give us the mean cloud observed. The mean cloud has a base at 1032 m and a vertical extention of 533 m. The last factor used for tuning against the model is the mean pyrgeometer flux of upwelling and downwelling longwave measurements 297.0 W/m^2 and 252.5 W/m^2 respectively, for the total group of clouds.

To set up the model with a cloud as similar as possible to the mean cloud, it was run with the Arctic autumn profile. This is because this profile was found to best represent the annual collected dataset. Initial run without a cloud was done for a clear sky. Comparing model clear sky fluxes with those observed give an estimated cloud longwave forcing of 68 W/m^2, in

close agreement with observed cloud forcing of 69.12 W/m^2. This suggests that the autumn profile is close to the annual average observed profile.

Comparison of model layer 24 with bottom 909.4 hPa and top 848.0 hPa with a radiosonde balloon[3] give the altitude of these pressure surfaces as 909.2hPa = 882m and 848hPa = 1440 m. For the 'Model' results of table 5.3, 769.4hPa = 2211m marks the top of the cloud. To get a cloud at this altitude to have as similar forcing as possible to the mean observed, LWP was tuned following the observed r_e of Garrett and Zhao (2006) of $r_e = 12.9\mu m$, and found to be close at $17g/m^2$. Then the model was then run for several different r_e.

Table 5.3 presents the combined results from observations and 1-D model, as well as a comparison with the results of Garrett and Zhao (2006). The model clouds are made so as to have as similar cloud base height and surface forcing as the observed cloud, and r_e was was then set from the basis of Garrett and Zhao (2006) observations. As described, the autumn profile was chosen to be most representative for the clouds. Based on this, a change in surface forcing was suited to observations from changing r_e and the remaining results deduced from this.

From table 5.3 it is also clear that the model results present a microstructure of the clouds that would explain the increase in surface forcing in terms of a cloud emissivity effect. The low CDNC and the LWP's of the model places the cloud sensitivity at $S_{LW} = 1.8$ $[\%cm^{-3}]$ (figure 2.4), which is among the most sensitive clouds. This shows that the observed increase may best be explained by a cloud sensitivity effect.

In this section the resulting increase in surface longwave forcing of increased CDNC in clouds has been presented. Incorporated model results and climatological properties has been presented and annual estimates obtained. The observed increase in surface longwave forcing, as a result of increased CDNC, has been shown to very likely be a cloud emissivity effect. The following section will present a discussion, as well as further evidence that what is observed is an emissivity effect.

5.4 Discussion

This section is in two parts. The first part is views on some of the results not previously discussed and the second part is in full focused on justifying the metods used. With precariously little detail on cloud microstructure this is an important part, and many possible influences are investigated, to ensure that the results obtained is indeed a cloud emissivty effect, and not other

[3]Surface pressure was on Aug.23'rd 2010 at 12:00, the time of release, 1011.7 at 11m, the AWI site in map 4.1

Results with model input

Properies/Variable	Observed thin	Observed	Model thin	Model	Garrett
CBH m	1032	969	882	882	500-3000
CVT / CT m	542	NA	558	1329	NA
LWP g/m^2	NA	NA	17	30	32.2 (31.1->33.5)
LWD W/m^2	251.8	282.0	246.2	263.1	NA
LWU W/m^2	301.2	300.4	270.4	270.4	NA
CF W/m^2	69.1*	72.5*	70.6	89.5	NA***
$\Delta SLCF$ W/m^2	3.57	1.74	3.5	1.75	3.3-5.2
r_e μm	NA	NA	13->11.2	13->11.1	12.9->9.9
Cloud albedo effect W/m^2	NA	NA	-2.35**	-2.80**	NA
Δ LW TOA W/m^2	NA	NA	-.05	-.09	NA
CDNC cm^3	NA	NA	3.7-6.1	3.3->5.4	53->153

Table 5.3: Summarized results. 'Observed thin' are the low thin clouds described in section 4.3, and 'Observed' are the low clouds. 'Model thin' is the best estimate for clouds similar to 'observed thin' and 'Model' a cloud thought to resemble 'Observed'. Garrett is the results of Garrett and Zhao (2006). When no information is available, column value NA, 'not available' is used. *estimated against annual average clear sky observations. **Model modifications applied, see discussion below. ***Compared to SHEBA of $65 \pm 10 W/m^2$ (Shupe and Intrieri, 2004)

influences on the observed forcing.

The increase in surface cloud forcing accredited a cloud emissivity effect of 3.57 W/m^2, the annual estimates and the higher than annual time resolution are summarized in table 5.1 and 5.3. The model inputs show that the mean cloud is most probably very sensitive. Following is a discussion on what other results were discovered. First the TOA forcing is considered followed by the other aspects presented in table 5.3.

The TOA forcing is highly dependent on the atmospheric profile used in the model. In the summer[4] and autumn profiles the atmosphere is cooler than the surface, thus a negative but small TOA longwave forcing. During winter the cloud can be warmer than the surface in the model and thus may have a positive TOA longwave forcing. That there is very little influence at TOA in the modelled results is in part due to the fixed surface temperature of the model, and therefore, studying TOA forcing in this regard is perhaps not as interesting.

The CDNC for the model and that of Garrett and Zhao (2006) is significantly different. From Garrett and Zhao (2006) it is clear that the clouds had a CVT of only $\sim 50-60m$ one order of magnitude thinner than those of the model and r_e is therefore also different.

How exactly the mean clouds in the clean and polluted cases differ is somewhat unknown. The mean aerosol number $[70-500nm]$ for the clean and polluted quartile is $N = 154cm^{-3}$ and $N = 2340cm^{-3}$ respectively. The mean vertical thickness of all the clouds are 542m. A hypothesized cloud with $LWP \sim 25\ g/m^2$ and $r_e = 20\mu m$, for the thin low clouds gives $r_e = 8.02\mu m$ for the high aerosol cloud group, following equation 2.12. This is based on a linear relationship between the number of aerosol available and the number of droplets activated. Based on table 5.3 activation is clearly not linear because the model show a much smaller increase in CDNC. The model result is suggestive for the difference in r_e of clouds formed in clean and polluted air.

Longwave model results are from autumn profile run for 15'th October, with a gas profile of Arctic October. In the shortwave some adjustments had to be done to estimate the Twomey effect. Since the magnitude of Twomey is strongly dependent to the magnitude of shortwave fluxes, the annual average shortwave global (section 4.1) was found to be slightly negative. Based on this and the annual albedo measurements of 0.46, the julian day of the year 245 was found to have the closest to the mean magnitude of shortwave. This time of year (Sept. 12th) is outside the domain of the October gas profile of the model, but this should not be a major source of error due to the small absorption of shortwave by gases.

[4]Neither summer nor winter results are shown

The cloud albedo effect in table 5.3 has about the same magnitude as the cloud emissivity effect. For the thin clouds, in terms of surface forcing, the longwave cloud emissivity effect is the larger at 3.5 W/m^2 as opposed to the shortwave albedo effect of -2.35 W/m^2. So that net surface forcing is positive. For the thicker clouds the net surface forcing is negative. Together these show that for the thinnest clouds it is actually the cloud emissivity effect that is the larger, but when increasing cloud LWC it no longer dominates.

Clouds especially selected for their sensitivity reveal a similar $\Delta SLCF$ to that observed by Garrett and Zhao (2006) and Lubin and Vogelmann (2006). This substantiate the theory of a prominent cloud emissivity effect in the Arctic. Appliance of model estimates reveal that most probably the clouds selected by the method of 4.3 are very similar to those of these studies.

Neither of the 2006 papers by Garrett and Lubin present any explicit frequency of the selected sensitive clouds or estimate an annual average. Therefore the suggested appliance (table 5.1) to annual potential is not transferable to these studies.

In this section, other possible influences than an emissivity change has been investigated and discussed in light of the modelled results. It was found that the cloud emissivity effect is larger than the cloud albedo effect for the thinnest group of clouds ($LWP <\sim 40 g/m^2$). The CDNC is very low for the clouds in the model, having one order of magnitude fewer $drops/cm^3$ than those of Garrett and Zhao (2006). The reason for this is that CVT in the study by Garrett and Zhao (2006) have one order of magnitude smaller CVT.

5.4.1 Validation

The prime concern of this section is to see what other aspects of the cloud properties that may influence results and as far as possible quantify it. There are many cloud properties that determine cloud surface forcing and thus must be investigated. Where possible it is measured and possible influence discussed.

The annual results have statistical strength in their large numbers. This is also needed since the variations in the surface fluxes are one order of magnitude larger than the observed quantities. Thus many of the examples shown have shorter timescales (fewer observations) to investigate their influence.

Figure 5.11 shows the LWD fluxes against surface skin temperature. Based on model results the red and blue line are approximated by using model results from the one dimensional model. The difference set out by a cloud of LWP of $100 g/m^2$ in level 25 of the model.

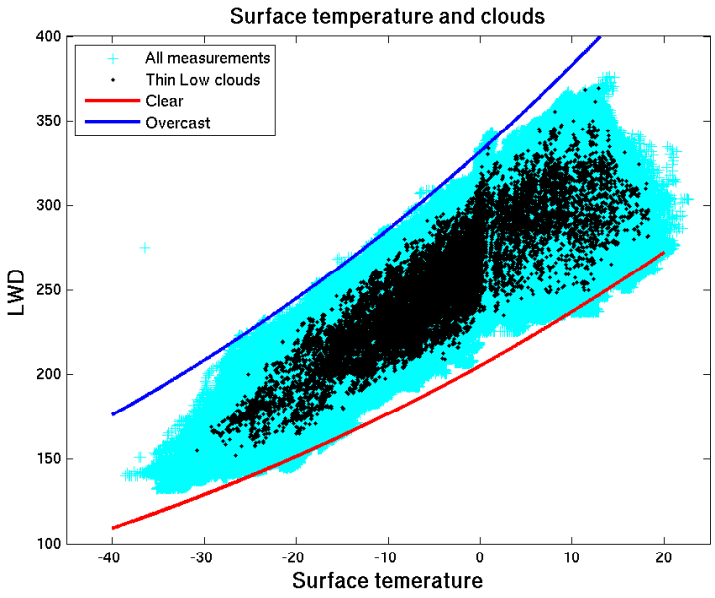

Figure 5.8: Shown here are the surface skin temperature estimated from radiative fluxes against downwelling longwave fluxes. Light blue is all observed instances. Black are the cloudy observations of 25 percentile optically thin clouds with cloudbases 0.6-2km. Lines indicate LWD fluxes expected with standard atmospheric components for clear and overcast conditions based on model results Blue: Based on model estimates for cloud in lvl 24-22 with LWP 100 g/m^2. Red: Based on model estimated clear sky

The black dots show that the low optically thin clouds lie in between these lines showing that they most probably have a LWP smaller than this. The reason very few measurements are included below $-25°C$ may be that it does not get colder than this in the presence of low clouds. Since these are instantaneous fluxes it may also be explained by the surface heat capacity in that it takes some time for the surface to cool this much and a strong stable layer must be in place to produce so extreme conditions.

Figure 5.11 shows that there is little reason to doubt that the selection process found clouds of low LWP. It also shows that these clouds may exist at all temperatures which has important implications to their frequency. That these clouds are found at the entire Arctic temperature range show that thin clouds may not be infrequent.

Multiple cloud layer influence

From figure 5.3 b) it is clear that there may be clouds present even with surface temperature well below $-25°C$. In all probability these are higher clouds. These higher clouds may also influence results if they are above a

lower cloud layer, especially if that cloudlayer has emissivity lower than unity. In most instances this are the high cirrus clouds normal to this region (Devasthale et al., 2011) The percentage time with multiple cloudlayers is much higher than those observed in figure 5.3 a). The reason for this is that the selected clouds are those where the MPL penetrate the cloud and thus are able to observe the clouds above.

Since clouds above influence the fluxes below a thin cloud, they have a potential to be a part of the observed signal of 3.57 W/m^2, but only if the clouds above differ between the clean and polluted clouds. When comparing the two set of data, if one have many multi-layer clouds and the other not, the result would be affected. An investigation of height and frequency of higher level clouds show, for the second level of clouds, a mean level two cloud base (CB2) CB2=5248m (78 %) & CB2=6384m (84 %) for high and low aerosol group respectively. A standard t-test for difference give only a p value of .65, indicating that these are variable and not significantly different. The frequency of observed clouds is indicated in brackets. The reason there are many more clouds above these clouds than indicated by figure 5.4 is that these are the clouds the MPL actually can detect clouds above.

A higher frequency of clouds above the clean quartile data increase LWD and so decreases the observed $\Delta SLCF$. A higher cloud base of the clouds above the clean quartile data should decrease LWD (adiabatic cooling with decreasing pressure) and thus increase $\Delta SLCF$. Based on this there is no evidence that the higher level clouds influence our estimated $\Delta SLCF$.

Cloud location

In limiting the clouds by having a cloud base between 600m and 2000m it was ensured that these clouds are affected by the aerosol numbers measured at Zeppelin mountain. Assuming an adiabatic lapse rate underneath the clouds, the clouds should have a similarly different temperature than that of the surface. For cloud longwave forcing the cloud temperature is very important and this again is very dependent on its altitude (e.g. Mauritsen et al. (2011)).

In figure 5.9 the regression show that the results should indeed be dependent on the location of the cloud base. A higher cloud base gives a smaller forcing within the domain. For a linear regression an estimated decrease of -12.2 $W/(m^2km)$ was found for the dataset. If comparing two dataset of assumed equal CBH, any difference in CBH may significantly influence results.

The MPL data gives no indication of cloud LWP other than the two rough groups, "can see through" and "cannot see through" which is close to a LWP of about $40g/m^2$. This means that within the group "can see through" there

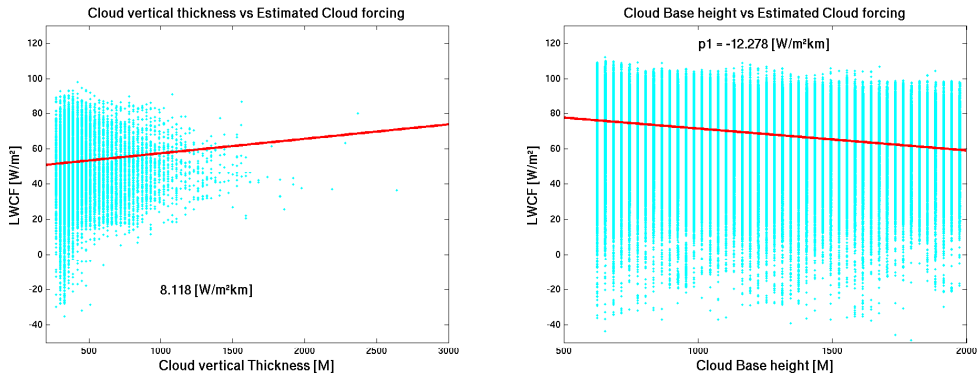

Figure 5.9: Regression analysis (red) using linear MRSE of a) Cloud vertical thickness and b) Cloud base height. LWCF is estimated by comparing standard Arctic atmospheric longwave fluxes to instantaneous pyrgeometer fluxes. It is thus only an indication of the real longwave forcing of the cloud. Datapoints is for all clouds with CB 600-2000m thin enough for the MPL to register a cloud top(46395 datapoints)

may be clouds of significantly different LWP. The closest thing to this is to look at the cloud's vertical extent, assuming that LWC does not vary greatly for clouds of different vertical thickness, the vertical thickness can be used as an estimate for LWP. Figure 5.9 gives a strong indication that cloud vertical thickness plays a role in increasing LWP, though a weaker signal than CBH, at 8.1 W/m^2km, and hence this may also strongly influence results.

Using only the clouds of LWP $<\sim 40g/m^2$ has the advantage that these statistics may investigated. For clouds of LWP so large that the MPL cannot penetrate, the vertical extent remains unknown when comparing two dataset. For the seasonal and monthly results there are much fewer data and they are hence more exposed to the natural variance of the dataset.

Annually, the polluted CBH $1104m$ & CVT $464m$ and the clean CBH $1048m$ & CVT $466m$, being nearly identical, should have no effect. Subdividing the data in seasonal or monthly subsets (figure 5.10) show that there are significant differences in the CBH and CVT of the polluted and clean clouds so that it may be interesting to look into detail on what this effact may be. From the regression analysis of figure 5.9 a formula for adjusting this analysis can be applied:

$$\Delta SLWCF_{adj} = \Delta SLWCF + CB_{diff} \times p1 + CVT_{diff} \times p2 \quad [W/m^2] \quad (5.4)$$

Here $\Delta SLWCF_{adj}$ is the adjusted value with regards to differences in CVT and CBH between the polluted and clean clouds. p1 and p2 are the first

order regression parameters of figure 5.9 and CB_{diff} & CVT_{diff} are the difference CB and CVT in kilometers between the polluted and clean clouds.

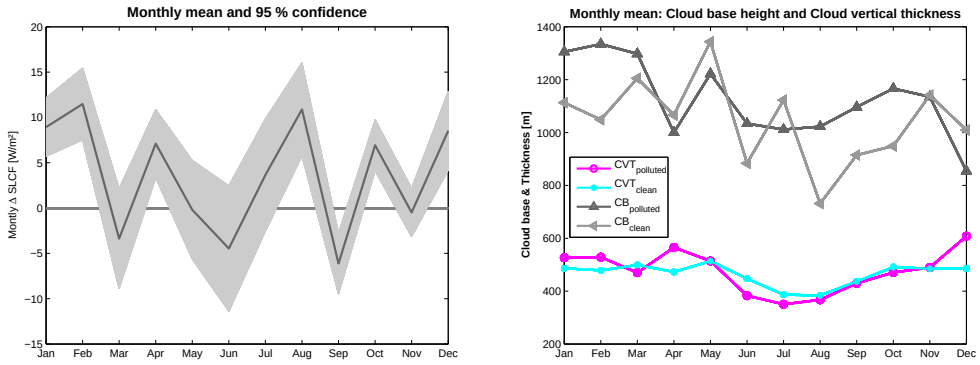

Figure 5.10: Left: Longwave monthly forcing with 95% confidence interval using quartile aerosol distributions. One month, September, stands out having with high confidence a negative forcing effect. Right: Cloud vertical thickness and cloud base height for each month. While minimal differences on annual results, comparison of monthly means show that differences in vertical structures in the cloud may influence results due to fewer samples.

From table 5.4.1 it is clear that, when getting fewer data, there is stronger influence on surface forcing by cloud location, even within the altitudes of cloud selection. The unphysical values are to some extent corrected by taking these altitudes into account by the use of equation 5.4. An interesting point to be made of this is in the seasonal[5], where autumn negative mean value is slightly positive when using this correction basis.

From analysis of how altitude differences influence results (figure 5.10), it is clear that when differences between the polluted and clean clouds are considered, the altitude of the clouds must be taken into account. From this analysis it is also clear that annual result for $\Delta SLWCF$ obtained here is not caused by such differences.

Ice influence

Very few observations of cloud ice content exist for the Arctic. Ice crystals are irregular in shape and this makes scattering and absorption coefficients harder to parametrize. Increased aerosol number densities increase the number of ice nuclei (IN), but less is known about IN than of CCN.

[5]indicated in table 5.4.1 by horizontal lines

Monthly Estimated forcing Corrected for CB and CVT

Month	$\Delta SLCF\ W/m^2$	CB_{diff} (m)	CVT_{diff} (m)	$\Delta SLCF_{Adj}\ W/m^2$
Jan	8.92	192.2	40.3	9.99
Feb	11.48	285.7	49.8	13.19
Mar	-3.37	92.6	-28.9	-2.26
Apr	7.11	-66.1	92.7	5.43
May	-0.19	-121.6	0.4	-1.18
Jun	-4.45	150.0	-64.5	-2.44
Jul	3.64	-111.8	-36.1	3.17
Aug	10.89	291.2	-16.6	13.46
Sep	-6.12	181.5	-6.9	-4.56
Oct	6.93	217.3	-20.3	8.95
Nov	-0.48	-5.6	4.8	-0.59
Dec	8.52	-155.1	122.3	5.76

Table 5.4: Monthly $\Delta SLCF$ estimates. Cloud Base (CB) and cloud vertical thickness (CVT) is given as the difference from the annual mean result for the combined quartile distribution. An indication that differences in CBH and CVT may influence the shorter period results. Adjusted is the adjusted monthly mean for CVT and CBH differences by equation 5.4. Note that each month contain different number of observations.

One approach would be to investigate ice water path (IWP) of the polluted and clean clouds, but as there is no information on either LWP or IWP of the clouds, so this is not possible for this set of data. Based on the findings of Devasthale et al. (2011), also described in section 3.3, a possible investigation of ice influence may possibly be examined by having a surface temperature cut off at e.g. $\sim -15°C$. Then the coldest cloud where most ice is expected is eliminated. When removing the samples having surface temperatures below $-15°C$ the annual estimate of $\Delta SLCF$ is $-3.46 W/m^2$ a decrease in estimated mean $\Delta SLCF$ of $0.11 W/m^2$.

The decreased results does not necessarily imply that the effect is larger for clouds with higher IWP. The strongest observed $\Delta SLCF$ is during winter, and removing many of these samples reduces the mean. Whether the observed larger cloud emissivity effect in winter is due to more clouds containing ice or have other reasons is not possible to deduce from the data. From the findings of Devasthale et al. (2011) it is probable that many of the clouds included contain ice, even when surface temperatures are above $-15°C$, and therefore it is hard to conclude what contribution IWP has.

Even though ice were found in most clouds, Devasthale et al. (2011) found that as many as 60% of the clouds contain liquid water at cloud base temperatures as low as $-20°C$, and this should ensure that most of the clouds observed are liquid or mixed-phase clouds.

Dependency on selection

Having shown results from the quartile (25%) and above/below median (50%), the results support the theory in that the clouds having the largest difference in emissivity are the ones with a large difference in CDNC. This is because the largest difference in SLWCF were observed by compairing the quartiles. Therefore, investigating other clean and polluted thresholds may be of interest.

On average using larger aerosol percentiles give lower average difference in SLWCF, but as shown in table 5.1, can give higher annual estimates. This is because of the restriction in LWP when defining thin clouds ensures that most clouds should be sensitive. To investsigate this a comparison of smaller percentiles was conducted in the same way as in section 5.3.

Results from this show that in fact the quartile results are the strongest. At 5% resolution (not shown) it is no significant trend that the intervals within the 0-25% domain[6] have a stronger S$\Delta SLCF$ towards the ends. Within the next domain 25-50 % the results are weaker ($[-0.07\ 0.31]\ W/m^2$) but there are no statistical significant results. Over all, when having too few data, the uncertainties increase because of the large variances in the fluxes.

5.4.2 Origin of airmasses

The online HYSPLIT model uses NCAR/NCEP reanalysis meteorology to determine Lagrangian particle trajectories. It can be run forward or backward in time and can use either a deterministic (high resolution) or ensamble version. (Draxler et. al. 2011 & Rolph et. al. 2011)

In the aim of investigating the origin of air that produce different aerosol conditions HYSPLIT was run for especially persistent low aerosol concentrations, and for the 10 highest aerosol concentrations.[7] Long periods for low aerosol concentrations were chosen, rather than the lowest concentrations, because it is believed to be more accurate. For the highest concentrations, which tend to be more spike like in behavior, this was not deemed a good approach.

Figure 5.11 shows two examples of many runs performed. In the instance of these two examples it seems clear that the clean sample (right) have been scavenged by rapid lifting in a front system and hence have few aerosol. The polluted sample (left) on the other hand, is probably loaded aerosol from the time at the surface east of Svalbard. Here there are no anthropogenic

[6] Where the total difference in SLWICF was $[3.21\ 4.87]W/m^2$

[7] This was for the period 2004-2010 since there were no older reanalysis files than this available in the HYSPLIT reanalysis files.

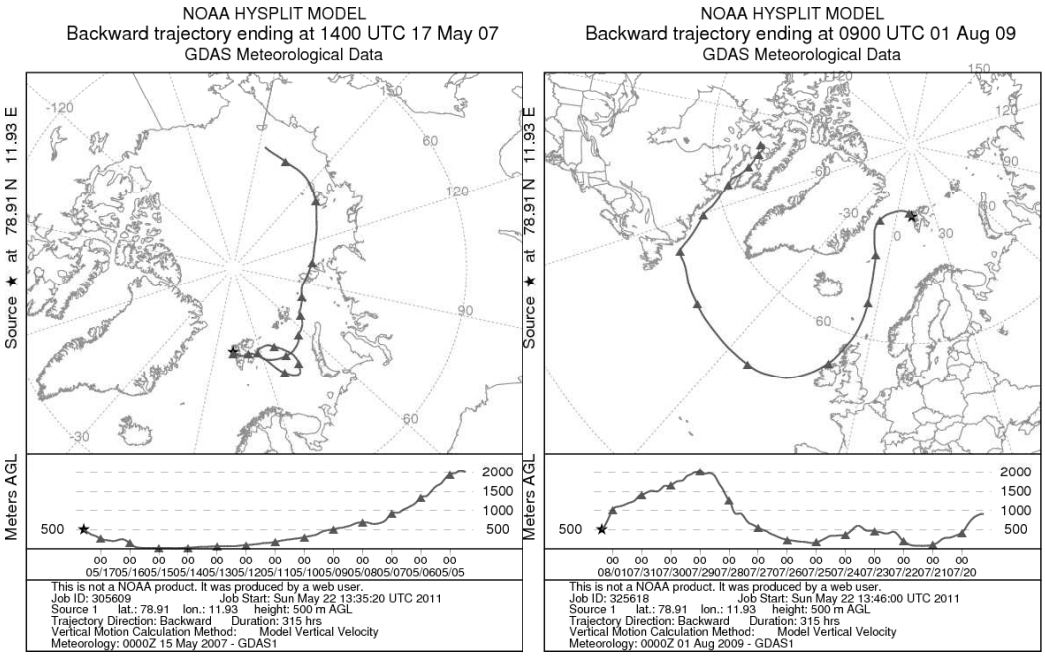

Figure 5.11: Example of HYSPLIT backward model run for a instance of particularly many accumulation mode aerosols (left) and a persistent instance of few accumulation mode aerosols (right). This may indicate that recent residence near surface may be as important as region, for having many accumulation mode aerosols. Bottom is the parcel altitude and top its location.

aerosols sources and thus it seems unlikely that this instance of polluted air can be explained only by anthropogenic sources. This example was chosen to show that transport patterns are complex and that more extensive reaserch like that of Hirdmann et al. (2011) is needed to establish certainties.

From figure 5.2 it is clear that the dominant wind direction is South Easterly, but this may as well only reflect the geographical location in the fjord as indicating the large scale motions.

The results of this investigation was inconclusive. No specific region of one or another type of instance could be pointed out as sources for the air measured. Residual times in the Arctic region was however longer on average before the low aerosol observations than for the high. The reason for the lack of definite results of this investigations may be due to HYSTAT inaccuracy or the complex picture of transport. The best indications on source regions and profiles remains from Hirdmann et al. (2011), but are more general than what was desired to obtain here.

5.4.3 Trends

Trends in the dataset are interesting, since they may point to the future. It is also a potential source of error in that selection from a trended distribution may result in a non representative selection. Therefore an investigation of the separate observations and their trends and what implications it has is necessary. From most data a trend was invariably found and its importance must therefore be consedered.

Hirdmann et al. (2011) also have investigated sensitivity for Zeppelin, and the most sensitive regions in terms of anthropogenic pollution being Europe and North America. The recent decrease in pollution in these regions may explain the decrease in observed accumulation mode aerosols from 2000 to 2010. That the long range accumulation mode aerosols have a stronger decreasing trend than the small support this.

The decrease in RH (figure 5.2) is interesting in that it influence the LCL. Because of this, a decrease in RH would potentially lead to, on average, higher cloud bases. Interestingly this is not an observed trend. CBH of clouds above NYA did not have any observable trend. This may have its source in that the CBH is connected to the mountanious geography around NYA, and that the RH measured at the surface has little influence on cloud formation.

A trend in cloud emissivty effect could not be observed with the metod used here. An investigation on the average year selected for the clean and polluted clouds show a small difference in the average year. For the clean the average year was 2006.6 and for the polluted 2006.7. That the polluted are on average drawn later from the dataset timeseries indicate that the observed trend of a decrease in accumulation mode aerosols may not be influential for the observed properties. Therefore it was done nothing to adjust for this trend when calculating percentiles.

In the first part of this section the results were discussed and put in their context. Results from model show that the surface forcing observed does not necessarily constitute a TOA forcing. Differences of the research by this thesis and previous work is discussed and the possible reasons put forward. In the validating part of this section, possible influences on results are discussed. Influence on surface forcing by cloud altitude, multiple cloud layers and ice influence were investigated and discussed, before an investigation of possible aerosol sources was conducted. From this discussion some conclusions may be made and these are presented in chapter 6.

Chapter 6

Conclusion

That clouds are an important driver of the Arctic climate has been established by much research (e.g. Initieri et al. (2002a)). Due to high surface albedo, long dark periods and low sun angles, longwave forcing by clouds is the dominant forcing by clouds in the Arctic. This is also true for NYA, where low thin clouds were found to increase longwave downflux compared to clear sky with 69 W/m^2.

Results presented in this thesis are the product of work done on a dataset which was perhaps not ideally suited to investigate the properties of interest. The main limiting factor was found to be the lack of accurate cloud readings in the set of data. The strength of the data however, was the long time series that allowed a statistical approach in analyzing the data. With the implementation of a 1-D model, most initial limitations were surpassed, and valid results were thereby obtained.

In accordance with the theory established by Garrett et al. (2002), it was found that for selected cases of thin low clouds above NYA, the quartile of most polluted clouds increased surface forcing by $[3.21 - 4.87]$ W/m^2 compared to similar clean clouds. This is in close accordance with results obtained by Lubin and Vogelmann (2006); Garrett and Zhao (2006) based on data from Barrow (Alaska). Table 5.3 reveals that the modeled microstructure of the clouds above NYA differ by an order of magnitude, in terms of CVT and CDNC, to those at Barrow. This places the clouds in the most sensitive region in figure 2.4. The method used in this thesis to investigate cloud emissivity effects follow established methods (Garrett and Zhao, 2006), albeit accommodating to the instruments available.

The strongest annual forcing was found when investigating clouds not limited by any vertical thickness restraints. The obseverd increase in surface forcing of these clouds was $[0.24 - 0.29]$ $W/(m^2 y)$. This means that the MPL cutoff must exclude many clouds which are sensitive or that there is a large LWP effect. Differentiating these effects is not possible for the low clouds with the method applied here. The decreased instantaneous surface forcing

of $[1.59 - 1.89]$ W/m^2, compared to the most sensitive clouds, implied that many clouds that are not sensitive were also included when limiting by the MPL's ability to penetrate the clouds. This number is likely to also include lifetime and increased LWC effects.

Several key elements that determine cloud influence on surface radiation were examined. Not only is the CBH important (-12.28 $W/(m^2km)$) but also the cloud vertical extention (8.12 $W/(m^2km)$) influence the observed surface forcing of clouds. Ice content and clouds above were examined and show a need for clearer measurements on cloud microstructure. Largely these effects were ruled out to have influenence on the main results.

The selection of the most sensitive low clouds and the annual estimate, contributed to show that clouds with emissivity lower than unity may be so infrequent at NYA that the modeled annual pan-Arctic estimate (Alteskjær et al., 2010) of $[0.1 - 0.85]$ W/m^2 is in fact in close accordance with the instantaneous values observed.

Seasonal (monthly) estimates were also investigated. However, as a result of fewer data, larger uncertainties make it difficult to reveal any affirmative evidence to seasonal (monthly) differences. Discovering seasonal differences would be important in order to see whether the longwave surface forcing from clouds is sufficient to perhaps amplify sea-ice loss at certain times of year. In many regions of the Arctic, a summer warming may also induce a permafrost thaw.

The observed decrease in aerosol number concentrations at Zeppelin since 2000, is consistent with other research (Hirdmann et al. (2011)). Case studies of instances with clean and polluted air done in this thesis revealed that there are complex mechanisms of transport and removal processes, reaching beyond the scope of this thesis, determining the accumulation mode aerosol numbers at NYA. Another study, (Hirdmann et al., 2011), reveals that Northern Europe and North America are the most important sources of anthropogenic aerosol at NYA. In this it is also important to note that the pollution in the polluted quartile does not necessarily mean that the aerosol has anthropogenic sources.

Changes in climatology (figures 5.1 & 5.2) in NYA show significant warming. For cloud formation it is also important to note that relative humidity is decreasing. The decline in RH (figure 5.2) would theoretically give a higher lifting cloud condensation altitude and on average higher clouds. From this, the expected trend of increasing CBH is not observed in the cloud data of this thesis.

Although the instruments at NYA are as stated not especially suited to investigate cloud microstructure, this has been discussed (sections 4.1 and 4.2)

and accounted for in the methods utilized. Arguments that the observed results using the method of this thesis is due to a cloud emissivity effect have been presented (section 5.4) together with incorporated 1-D model results (section 5.3.3). In conclusion, the results presented in this thesis support the main hypothesis , that there is a sizable cloud emissivity effect in clouds above NYA. Whether or not these results are generalizable to the whole of the Arctic region requires further research.

6.1 Further reasearch

The results presented in this thesis provide new insight into the cloud forcing mechanisms in the Arctic. If further progress concerning cloud forcing mechanisms is to be achieved based on NYA observations, there is a need of new and more specified instruments for cloud microstructure measurements. A multichannel Lidar combined with mm radar seems the obvious choice for investigating cloud microstructure. This would yield information on water phase, droplet size distribution and temperature profiles in addition to what is already known.

A more advanced instrument park with enhanced cloud detection techniques would vastly increase the knowledge of the clouds above NYA. As NYA is one of the very few permanent Arctic research stations, this would also increase our knowledge of Arctic clouds in general. Better cloud detection techniques would help effectively determine cloud lifetime, LWC and pure emissivity effects.

Another line of research which should be pursued is the NYA sources of aerosol pollutants. This is probably best done using a modeling tool. Source profiles, source regions and transport patterns must be identified for the aerosols to be able to evaluate the anthropogenic contribution to the observed surface forcing. Chemical analyses of the aerosols are important, both with regards to how aerosols interact with clouds, as well as how aerosol behaves in the atmosphere.

As a result of the findings of this thesis, an important line of research could be to take a closer look at feedback-mechanisms between the clouds and the surface (Tietze et al., 2011). The calculations of this thesis are an instantaneous surface forcing in a localized region, not a TOA global forcing. Important questions for further research therefore include: Will local albedo decrease with an increased surface cloud forcing? How can this in turn change cloud forcing? Local feedback mechanisms is probably the most vital path to follow in order to find the most important consequences of the cloud emissivity effect. This thesis has provided ample grounds for further research within cloud longwave forcing sensitivities which may lead to a greater understanding of clouds as a driver of Arctic climate.

Appendix A

Statistical methods

In this appendix the statistical methods used for calculating data averages and variances are included. To format data from one minute average and variance data to one hour mean value and variance data, statistical expectation and variance is used. Also included is a description of statistics fo confidence ranges and mean values for results are procured.

In 1993 a US supreme court ruling it was stated that: `''Between two and three standard deviations from a normal distribution should be the standard for accepting scientific evidence`[1]`.''` Following this reasoning a statistical significance level of 95% is used throughout this thesis, unless otherwise stated.

The expected value of N samples is given by the mean value:

$$E(X) = \frac{1}{N}\sum X_i \tag{A.1}$$

Where N is the total number of samples and X_i a spesific sample value.
Most instruments have a faster sample rate than one minute so the expected value is actually the sum of many expected values. If we assume that each of the datasets minute long observations contain the same number of observations, the combined expected value of the M expected values are:

$$E(E(X)) = \frac{1}{M}\sum_M E(X_j) = \frac{1}{MN}\sum_M\sum_N X_{ij} \tag{A.2}$$

The variance of N samples is given by:

$$Var(X) = E((X - E(X))^2) = \frac{1}{N}\sum_N (X_i - E(X))^2 \tag{A.3}$$

For a dataset X of M independent subsets each with N samples in each and mean and sample expected value and variance $E(X_j) = \mu_j$ & $Var(X_j) = S_j^2$

[1] Daubert v. Merrell Dow Pharmaceuticals, 509 U.S. 579 (1993)

the variance of the complete dataset are given by combining the expected variances and the variance of the expected values:

$$Var(X) = Var(E(X_j)) + E(Var(X_j))$$

$$Var(X) = Var(E(\mu_j)) + \frac{1}{M}\sum_{M} S_j^2 \tag{A.4}$$

If we assume that each subset contains the same number of observations of equal precision, the hour long variance computation is simply:

$$Var(X) = \frac{1}{M}\sum_{M}(E(\mu_j) - \mu_j)^2 + \frac{1}{M}\sum_{M} S_j^2 \tag{A.5}$$

Thus the variance for the combined dataset is given by the variance of the minute long means plus the mean of the subset variances. The monthly averages and yearly averages are calculated aswell as the hour averages.

When calculating variance for pooled estimates that are not independent, their dependent variance, or covariance, must be subtracted to obtain the pooled variance. Radiative fluxes are dependent on each other as they measure exchange of energy, which in turn alter the rate of exchange. When adding two dependent variables their expected value is given by A.2 and their combined variance (Rice, 1994):

$$Var(X_1 + X_2) = Var(X_1) + Var(X_2) + 2Cov(X_1, X_2) \tag{A.6}$$

$$Var(X_1 - X_2) = Var(X_1) + Var(X_2) - 2Cov(X_1, X_2) \tag{A.7}$$

Where the covariance is given by:

$$Cov(X_1, X_2) = E(X_1X_2) - E(X_1)E(X_2) \tag{A.8}$$

Equation & are important because the estimates for surface cloud forcing or cloud emissivity effect is combined by four fluxes of energy:

$$SCF = F_P \uparrow - F_P \downarrow - (F_C \uparrow - F_C \downarrow) \tag{A.9}$$

Where P is polluted and C is clean and the arrow indicate the direction of radiation. Then using:

$$F_P^{Net} = F_P \uparrow - F_P \downarrow \quad and \quad F_C^{Net} = F_C \uparrow - F_C \downarrow \tag{A.10}$$

to get to the variance of SCF:

$$Var(X_H - X_L) = Var(F_P \uparrow) + Var(F_P \downarrow)) + Var(F_C \uparrow) + Var(F_C \downarrow))$$
$$-2(Cov(F_P^{Net}, F_C^{Net}) + Cov(F_C \uparrow, F_C \downarrow) + Cov(F_P \uparrow, F_P \downarrow)) \tag{A.11}$$

To calculate the covariance of two dataset of an unequal number of samples directly is impossible (Rice, 1994). The samples need to be paired to give any meaning, and for most estimates in this thesis, with few exceptions, this was not the case. The aproach used instead was to use ranked distribution statistics.

t-statistics

To use t or z-distribution statistics the underlying assumption is that the data comes from a normal distribution. If the sample distribution differs significanlty from the normal these tests are not valid.
When the sample distribution function can be well represented by the normal distribution these tests provide statistics for difference in mean. [2]
The t-statistics for two samples follows the t-distribution

$$t = \frac{\bar{X}_1 - \bar{X}_2}{S_{\bar{X}_1 - \bar{X}_2}}$$

Using statistical software or tables can give you maximum likelihood estimates for difference of mean and t-statistics confidence interval. In most instances there was a lower than 50% probability of estimate coming from a normal distribution and thus another option was to use statistics where no underlying assumption about the distribution of the data is needed, namely the Kolmogorov-Smirnov statistics.

Kolmogorov - Smirnov statistics

Kolmogorov-Smirnov (K-S) test is an empirical cumulative distribution function (ECDF) test that can be used to decide if two sample populations come from the same distribution. The ECDF of a dataset is defined as:

$$E_N = \frac{n(i)}{N}$$

where $n(i)$ is the number of points smaller than $X(i)$ where $X_1, ...X_i, ...X_N$ is the ranked datapoints. For two ECDF of n and m datapoints, $F_m(x)$ and $G_n(x)$ the Kolmogorov-Smirnov statistics is given by:

$$D_{mn} = (\frac{mn}{m+n})^{1/2} sup_x |F_m(x) - G_n(x)| \tag{A.12}$$

where $sup_x|F_m(x) - G_n(x)|$ is the maximum difference between the two ECDF. Based on the K-S probability function:

$$K(t) = 1 - 2\sum_{i=1}^{\infty}(-1)^{i-1}e^{-2i^2t} \tag{A.13}$$

and statistical software or tables, probability for the two coming from the same distribution given that (m, n) is large enough.[3]
This test can be applien both for two samples or for one sample and any distribution. It was used to test the observed results against a normal distribution aswell as for testing differences in mean. Though not ideal to test difference in mean, modified ECDF assuming equal variance can be applied to get maximum likelihood and confidence interval for difference in mean of two sample distributions.

[2] $http://en.wikipedia.org/wiki/Student\%27s_t-test$

[3] $http://ocw.mit.edu/courses/mathematics/18-443-statistics-for-applications-fall-2006/lecture-notes/lecture14.pdf$

Appendix B

Abbreviations used

Accumulation mode Large aerosol $> 70nm$
AERI Atmospheric Emitted Radiance Interferometer
Aitken mode Small aerosol $< 70nm$
AWI Alfred Wegner Institute

BB Beamblock

CALYPSO Cloud-Aerosol and Infrared Pathfinder Satellite Observations
CB(H) Cloud base (height)
CCN Cloud condensation nuclei
CDNC Cloud droplet number concentration
CF Cloud forcing
CPC Condensation Particle Counter
Clean Few accumulation mode aerosol
CVT Cloud vertical thickness
CT(H) Cloud top (height)

DMPS Differential Mobility Particle System
DMA Differential Mobility Analyzer

ECMWF European Center for Medium range Weather Forcasts

HYSPLIT online lagrangian particle tracer.

IN Cloud ice nuclei
K-S Kolomogorov- Smirnov

LIDAR Light detection and ranging
LWC Cloud liquid water content
LWD Longwave down
LWP Cloud liquid water path
LWU Longwave up

MPL Micropulse Lidar

N Number of aerosol
NASA National Aeronautics Space Administration
NCAR National Center for Atmospheric Research
NCEP National Centers for Environmental Prediction
NILU Norwegian Institute of Air Research
NP Norwegian Polar Institute
NYA Ny Aalesund/Ny Ålesund

Polluted Many accumulation mode aerosol

RADAR Radio detection and Ranging

SWD Shortwave down
SWU Shortwave up
SHEBA Surface Heat Budget of the Arctic Ocean
$\mathbf{S}_{lw}$ Sensitivity to longwave
SCF Surface cloud forcing
SLWCF Surface longwave cloud forcing
SSWCF Surface shortwave cloud forcing
SU Stockholmska University

t-test Student t-test

WMO World meteorological organization

Bibliography

Albrecht, B. A. (1989) *A*erosol, cloud microphysics and fractional cloudiness.. Science, Vol. 245: p. 1227–1230.

Alteskjær, K.; Kristjánsson, J. E. and Hoose, C. (2010) *D*o antopogenic aerosols enhance or supress the surface cloud forcing of the Arctic?. Journal of Geophysical Research, Vol. 115(D22204). Doi:10.1029/2010JD014015.

Beine, H.J.; Engardt, M.; Jaffe, D.A.; Hov, Ø.; ', K. Holmén and Stordal, F. (1996) *M*easuremnt of NOx and aerosol particles at the Ny Ålesund Zeppelin mountain station on Svalbard: Influence of regional and local pollution sources.. Atmospheric environment, Vol. 30(7): p. 1067–1079.

Caldow, R.C.; Palmer, M.R. and Quant, F.R. (1992) *P*erformance of the TSI Model 3010 Condensation Particle Counter. presented at the American Association for Aerosol Research Eleventh Annual Meeting; San Fransisco. Http://www.wmo.int/pages/prog/www/IMOP/meetings/MG-9/Doc-4-1(3)_WP-A3.doc.

Campbell, J. R.; Sassen, K. and Welton, E. J. (2008) *E*levated cloud and aerosol layer retrievals from micropulse lidar signal profiles. J. Atmos. Oceanic Technol., Vol. 25: p. 685–700.

Chen, Hongbin; Xia, Xiangao; Wang, Pucai and Zhang, Wenxing (2007) *G*round-based measurements of aerosol optical properties and radiative forcing in North China. China Particoulogy, p. 202–205. SienceDirect.

Clothiaux, Eugene E.; Ackerman, Thomas P.; Mace, Gerald G.; Moran, Kenneth P.; Marchand, Roger T.; Miller, Mark A. and Martner, Brooks E. (2000) *O*bjective Determination of Cloud Heights and Radar Reflectivities Using a Combination of Active Remote Sensors at the ARM CART Sites. J. Appl. Meteor., Vol. 39: p. 645–665. Doi: 10.1175/1520-0450(2000)039.

Curry, J. A. and Ebert, E.E. (1992) *A*nnual cycle of radiative fluxes over the Arctic ocean: Sensitivity to cloud optical properties. J. Climate, Vol. 5: p. 1267–1280.

Curry, J. A.; Rossow, W. B.; Randall, D. and Schramm, J. L. (1996) *O*verview of Arctic Cloud and Radiation Characteristics. J. Climate, Vol. 9: p. 1731–1764.

Devasthale, A.; Tjernström, M. and Omar, A. H. (2011) *T*he vertical distribution of thin feautures over the Arctic analysed from CALYPSO observations. Tellus B, Vol. 63(1): p. 77–85. Doi:10.1111/j.1600-0889.2010.00516.x.

Ellingsworth, J.; Welton, E. J.; Kenneth, J.; Gordon, H. R.; H.Maring; Smirnov, A.; Holben, B.; Schmid, J. M. Beat; Livingston, P. B.; Russel, P. A.; Formenti, D. P. and Andreae, M. (2000) *G*round-based lidar measurements of aerosols during ACE-2: Instrument description, results, and comparisons with other ground-based and airborne measurements. Tellus, Vol. 52(B): p. 635–65.

Feltz, W. F.; Smith, W. L.; Knuteson, R. O.; E.Revercomb, H.; Woolf, H. M. and Howell, H. Ben (1998) *M*eteorological Applications of Temperature and Water Vapor Retrievals from the Ground-Based Atmospheric Emitted Radiance Interferometer (AERI). J. Appl. Meteor., Vol. 37: p. 857–875. Doi:10.1175/1520-0450.

Garrett, T. J.; Radke, L. F. and Hobbs, P. V. (2002) *A*erosol effects on the cloud emissivity and surface longwave heating in the Arctic. J.Atmos.Sci., Vol. 59: p. 769–778.

Garrett, T. J. and Zhao, C. (2006) *I*ncreased Arctic cloud longwave emissivity associated with pollution from mid-lattitudes.. Nature, Vol. 440(D22204): p. 787–789. Doi:10.1038/nature04636.

Garrett, T. J.; Zhao, C.; Dong, X.; Mace, G.G. and Hobbs, P.V. (2004) *E*ffects of varying aerosol regimes on low-level Arctic stratus.. Geophys. Res. Lett., Vol. 31(L17105). Doi:10.1029/2004GL019928.

Hartmann, Dennis L. (1994) *G*lobal Physical Climatology (Academic Press). Ch. 4 pp.

Hirdmann, D.; Burkhart, J. F.; Sodermann, H.; Eckhardt, S.; Jefferson, A.; Quinn, P.K.; Sharma, S.; Ström, J. and Stohl, A. (2011) *L*ong-term trends of black carbon and sulphate aerosol in the Arctic: changes in atmospheric transport and source region emissions. Atmos. Chem. Phys. Discuss., Vol. 11(7). Doi:10.5194/acpd-11-8801-2011.

Initieri, J. M.; Fairall, C. W.; Shupe, M. D.; Persson, P. O. G.; Andreas, E. L.; Guest, P. S. and Moritz, R. E. (2002a) *A*n annual cycle of Arctic surface cloud forcing at SHEBA. J. Geophys. Res., Vol. 107(13): p. 1–13.

Initieri, J. M.; Shupe, M. D.; Uttal, T. and McCarty, B.J. (2002b) *A*n annual cycle of Arctic cloud characteristics observed by radar and lidar at SHEBA. J. Geophys. Res., Vol. 107(C10): p. 8030. Doi:10.1029/2000JC000423.

IPCC (2007) *S*ummary for Policymakers. In *C*limate Change 2007: The Physical Science Basis. Contribution of Working Group I to the Fourth

Assessment Report of the Intergovernmental Panel on Climate Change [Solomon, S., D. Qin, M. Manning, Z. Chen, M. Marquis, K.B. Averyt, M. Tignor and H.L. Miller (eds.)] (Cambridge University Press, Cambridge, United Kingdom and New York, NY, USA).

Ji, Qiang and Tsay, Si-Chee (2000) *O*n the dome effect of Eppley pyrgeometers and pyranometers. Geophys. Res. Lett., Vol. 27(7). Doi:10.1029/1999GL011093.

Kiehl, J. T.; Hack, J. J.; Boville, G.B.; Williamson, D. L. and Rasch, P. J. (1998) *T*he National Center for Atmospheric Reaserch Community Climate Model: CCM3. J. Clim, Vol. 11: p. 1131–1149.

Liou, K.N. (2002) *A*n Introduction to Atmospheric Radiation (2'nd edition) (Academic press).

Lohmann, U. and Feichter, J. (2005) *G*lobal indirect aerosol effects: a review. Atmos. Chem. Phys., Vol. 5: p. 715–737.

Lubin, D. and Vogelmann, A. M. (2006) *A* climatologically significant aerosol longwave indirect effect in the Arctic. Nature, Vol. 439: p. 453–456.

Martin, M.; Chang, R. Y.-W.; Sierau, B.; Sjogren, S.; Swietlicki, E.; Abbatt, J. P. D.; Leck, C. and Lohmann, U. (2011) *C*loud condensation nuklei closure study on summer Arctic aerosol. Atmos. Chem. Phys. Discuss., Vol. 11(7). Doi:10.5194/acpd-11-8801-2011.

Mauritsen, T.; J.Sedlar; M.Tjernstöm; C.Leck; M.Martin; M.Shupe; S.Sjogren; B.Sierau; P.O.G.Persson; I.M.Brooks and E.Swietlicki (2011) *A*n Arctic CCN-limited cloud-aerosol regime. Atmos. Chem. Phys., Vol. 11: p. 165–173.

Nishizawa, T.; Sugimoto, N.; Matsui, I.; Shimizu, A.; Tatarov, B. and Okamoto, H. (2008) *A*lgorithm to Retrieve Aerosol Optical Properties From High-Spectral-Resolution Lidar and Polarization Mie-Scattering Lidar Measurements. Geoscience and Remote Sensing, IEEE Transactions, Vol. 46(12): p. 4094–4103. Doi:10.1109/TGRS.2008.2000797.

Overland, James E.; Spillane, Michael C.; Percival, Donald B.; Wang, Muyin and Mofjeld, Harold O. (2004) *S*easonal and regional variation of pan-arctic surface air temperature over the instrumental record. J. Climate, Vol. 17: p. 3263–3282. Doi: 10.1175/1520-0442(2004)017.

Pincus, R. and Baker, M. B. (1994) *E*ffect of precipitation on albedo susceptibility of clouds in the marine boundry layer.. Nature, Vol. 372: p. 250–252.

Quinn, P. K.; Bates, T. S.; Baum, E.; Doubleday, N.; Fiore, A. M.; Flanner, M.; Fridlind, A.; Garrett, T. J.; Koch, D.; Menon, S.; Shindell, D.; Stohl,

A. and Warren, S. G. (2008) *S*hort-lived pollutants in the Arctic: their climate impact and possible mitigation strategies. Atmos. Chem. Phys., Vol. 8: p. 1723–1735.

Rice, John. A. (1994) *M*athematical Statistics and Data Analysis (Duxbury Press, Belmont California). Ch.3 pp 83-97,Ch.4 pp 129,Ch.7, Ch.8 pp 253.

Rogers, R. R. (1989) *A* short course in Cloud Physics (Butterworth - Heinemann). Ch. 4,5.

Seinfeld, John H. and Pandis, Spyros N. (2006) *A*tmospheric Chemistry and Physics - From Air Pollution to Climate Change (2nd Edition) (John Wiley & Sons). Online verison.

Shupe, M. D. and Intrieri, J. M. (2004) *C*loud radiative forcing of the Arctic surface: the influence of cloud properties, surface albedo, and solar zenith angle.. Journal of Climate, Vol. 17: p. 616–628.

Tietze, K.; Riedl, J.; Stohl, A. and Garrett, T. J. (2011) *S*pace-based evaluation of interactions between aerosols and low-lever Arctic clouds during the Spring and Summer of 2008. Atmos. Chem. Phys., Vol. 11: p. 3359–3373.

Twomey, S. (1977) *T*he influence of pollution on the Shortwave albedo of clouds. J. Atmos. Sci., Vol. 34: p. 1149–1152.

Vuerich, E. (1999) *C*ommission for instruments and methods of observation. Http://www.wmo.int/pages/prog/www/IMOP/meetings/MG-9/Doc-4-1(3)_WP-A3.doc.